Norwegian University of Life Sciences
Department of Ecology
and Natural Resource Management

Philosophiae Doctor (PhD)
Thesis 2017:19

Use of photogrammetric 3D data for forest inventory

Bruk av 3D-data fra fotogrammetri for skogtaksering

Stefano Puliti

Use of photogrammetric 3D data for forest inventory

Bruk av 3D-data fra fotogrammetri for skogtaksering

Philosophiae Doctor (PhD) Thesis

Stefano Puliti

Faculty of Environmental Sciences and Natural Resource Management
Norwegian University of Life Sciences

Ås 2017

Thesis number 2017:19
ISSN 1894-6402
ISBN 978-82-575-1425-9

PhD Supervisors

Professor Terje Gobakken
Faculty of Environmental Sciences and Natural Resource Management
Norwegian University of Life Sciences
P.O. Box 5003, NO – 1432 Ås, Norway

Professor Erik Næsset
Faculty of Environmental Sciences and Natural Resource Management
Norwegian University of Life Sciences
P.O. Box 5003, NO – 1432 Ås, Norway

Dr. Hans Ole Ørka
Faculty of Environmental Sciences and Natural Resource Management
Norwegian University of Life Sciences
P.O. Box 5003, NO – 1432 Ås, Norway

Evaluation Committee

Professor Hailemariam Temesgen
Department of Forest Engineering, Resources and Management
Oregon State University
280 Peavy Hall, Corvallis, OR 97331, USA

Professor Lars Torsten Waser
Landscape Dynamics Swiss Federal Research Institute WSL
Zürcherstrasse 111, 8903 Birmensdorf, Switzerland

Professor Tron Eid
Faculty of Environmental Sciences and Natural Resource Management
Norwegian University of Life Sciences
P.O. Box 5003, NO – 1432 Ås, Norway

Acknowledgements

First and foremost, I would like to thank my PhD supervisors and co-authors in all papers, Prof. Terje Gobakken and Prof. Erik Næsset. The work included in this dissertation is the result of their support with all possible financial and intellectual resources. I am very grateful for providing me with complete intellectual freedom in pursuing my research interests. The past three years have been an invaluable learning experience that will guide me and inspire me throughout my career. A special thanks also goes to my colleague Dr Liviu Ene, whom, in addition of being co-author in one of the papers, has been an irreplaceable source of ideas. I am thankful also to Dr Hans Ole Ørka for the supervision during my PhD and fruitful discussions. I wish to also thank Dr Svetlana Saarela and Professor Goran Ståhl, co-authors in one of the papers, for the valuable input in guiding me through the complexity of forest sampling.

I am also grateful to Prof. Johan Holmgren, Prof. Matti Maltamo, Dr Petteri Packalen, Dr Jari Vauhkonen, and Prof. Timo Tokola for introducting and mentoring me in my first steps into the use of 3D remotely sensed data for forest inventory. My gratitude also extends to Victor Strimbu, Dr Endre Hofstad Hansen, and Dr Ole Martin Bollandsås for rewarding discussions throughout my PhD.

To my friends here in Norway, I am extremely thankful for making this time in the land of Vikings so pleasant. Special thanks goes to Arnaud and Marta, who accompanied me in many adventures keeping me sane during the intense PhD work. To Pippo and Tommy, regardless the distance that separates us, our brotherhood has been and continues to be a pillar in my life. A very special thanks goes to Gregorio, you awakened in me an energy to pursue life that I was not aware I had.

To my partner, Megan, I am deeply grateful for your help in reviewing the language of my papers, for your love and understanding, you are truly inspiring. My deepest gratitude goes to my mother and father, who supported me throughout these never-ending studies with love, finances, and regular provision of olive oil. Thank you for believing in me and inspiring me to achieve ever higher goals.

Stefano Puliti

Ås, March 20, 2017

Contents

Abstract

Aerial imagery have long been used as auxiliary information to reduce the costs of forest inventories. Due to the high correlation between tree height and forest biophysical properties, manual photogrammetric techniques have been applied to aerial imagery for the measurement of vertical canopy structure, an important variable in forest inventories. In the past decade years, major advances have resulted in the development of photogrammetric software for the automatic generation of photogrammetric data from digital imagery. As a result, user-friendly advanced photogrammetric software are now available on the market, allowing for an increasing number of users to produce dense three-dimensional (3D) photogrammetric point clouds. The increased accessibility to advanced software in addition to the large availability of aerial imagery has led to a renaissance in the use of photogrammetry for forest inventory. The smaller costs of acquiring photogrammetric data compared to alternative 3D remote sensing data (i.e., airborne laser scanning; ALS), make their use appealing. The four studies included in this thesis addressed the use of photogrammetric data for the two main categories of forest inventories, namely: forest management inventories (FMI) and large-scale forest surveys (LSFS). For both categories, this thesis illustrated potential applications for which photogrammetric data may be advantageous over alternative 3D remote sensing data.

Wall-to-wall photogrammetric data produced from imagery collected using different platforms, i.e. a manned aircraft in paper I and an unmanned aerial vehicle (UAV) in paper II, were used to model forest biophysical properties of interest in FMI. Both structural and spectral variables from photogrammetric data were used as predictor variables. Furthermore, when available, accuracy figures from ALS based inventory were used as a benchmark. The accuracy assessment revealed that photogrammetric data were able to predict forest biophysical properties with similar accuracy to ALS data. Furthermore, the first two papers highlighted some advantages related to photogrammetry, namely: 1) the possibility to use spectral information for species-specific FMI, and 2) the versatility of acquiring photogrammetric data using UAVs.

Moreover, the possibility to use UAVs in forest inventories was further addressed by illustrating LSFS applications for which UAVs could be cost-efficient. As a means of reducing the costs for RS auxiliary data acquisition, UAV data were acquired as a sample (i.e. partial-coverage) over a large area. In paper III the sample of UAV data, together with a subsample of field data were used in a hybrid inferential framework to estimate growing

stock volume (GSV) and assess its uncertainty. Such an approach enabled an increase in precision compared to design-based estimates using only field data. In paper IV, these data sources were augmented by a third wall-to-wall layer of Sentinel-2 multispectral data as a means of further increasing the precision of the estimator. In the latter case, the recently developed hierarchical model-based inference was adopted to enable a statistically rigorous estimation of the GSV and its uncertainty. This approach resulted in a slight increase in the precision of the hybrid estimator. Nevertheless, it allowed for a reduction of the UAV sampling intensity, hence reducing the UAV acquisition costs substantially.

Overall, the thesis concluded that photogrammetric data will have an increasingly important role in forest inventories. Not only are comparable levels of accuracy achievable, but their use can be more cost-efficient than alternative 3D remotely sensed data. Even though further research in different forestry settings should confirm our findings, the applications described in this thesis were found to have potential for operational use.

List of papers

Paper I: Puliti, S., Gobakken, T., Ørka, H.O., Næsset, E. (2016). Assessing 3D point clouds from aerial photographs for species-specific forest inventories. *Scandinavian Journal of Forest Research*, 32, 68-79.

Paper II: Puliti, S., Ørka, H.O., Gobakken, T., Næsset, E. (2016). Inventory of small forest areas using an unmanned aerial system. *Remote Sensing*, 7, 9632.

Paper III: Puliti, S., Ene, L.T., Gobakken, T., Næsset, E. (submitted). Use of partial-coverage UAV data in sampling for large scale forest inventories.

Paper IV: Puliti, S., Saarela, S., Gobakken, T., Ståhl, G., Næsset, E. (manuscript).Combining UAV and Sentinel-2 auxiliary data for forest growing stock volume estimation through hierarchical model-based inference.

SYNOPSIS

1. Introduction

1.1 Aerial imagery

Aerial images have been and continue to be widely used in forest inventories as a means to reduce the overall inventory costs and to produce maps of forest resources. These represent the oldest source of remote sensing (RS) data (Wulder 1998). The first examples of the use of aerial images for forest inventory purposes date back to the 1920's in the United States (Seely 1929, Standish 1945, Taniguchi 1961). Further examples in Scandinavian countries are described by Korpela (2004a) and Packalén (2009). At that time, the possibility to obtain large coverage of auxiliary data offered opportunities to reduce the costs and time needed to inventory large forest areas (Standish 1945). The use of the bi-dimensional (2D) spectral information from aerial images has been largely applied to accomplish tasks of stratification to support more efficient sampling design in large scale forest surveys (LSFS) as well as for estimation purposes in forest management inventories (FMI) (Korpela 2004a). In FMI, there is a particular interest in the use of aerial images for modelling forest biophysical properties. Examples using 2D spectral data for estimation of forest biophysical properties can be found in Chiao (1996), Hyyppä et al. (2000). A drawback of using imagery for these tasks is that the relationship between 2D spectral information and forest biophysical properties such as growing stock volume (GSV) or height is often weak because of a lack of information on the vertical canopy structure. Because of this limitation, the accuracy yielded by forest inventories based on aerial images has typically been lower than that of traditional field based inventories (Packalén 2009).

1.2 Photogrammetry

Since the 1940's, soon after the first studies using 2D information from aerial imagery, researchers started looking into applying photogrammetric techniques to obtain three-dimensional (3D) information on the forest canopy (Taniguchi 1961, Korpela 2004a). Such techniques, aided by analogue stereo-plotters enabled the measurement of tree heights from image stereo-pairs (Baltsavias 1999). The importance of these 3D measurements in describing the forest canopy structure were rapidly acknowledged. As a result, photogrammetric measurements were included to support FMI (Næsset 1990, Næsset 1991, Eid and Næsset 1998). Because these measurements were carried out manually, only a coarse spatial representation of the vertical structure of the canopy could be produced. The advent of digital imagery enabled the automation of photogrammetric workflows allowing the shift

from scattered photogrammetric measurements to the concept of the point cloud, i.e. a set of continuous and spatially uniform 3D measurements. Digital photogrammetric software began to be developed in the late 1980's - early 1990's (Lohmann et al. 1989, Leberl 1994, Baltsavias 1999). Initially, the applications in forestry were limited but in the late 1990's and early 2000's, thanks to advances in computing, the potential for digital photogrammetric data for forest inventory increased (Halbritter 1996, Næsset 2002a, Korpela 2004a, Korpela 2004b). The study by Næsset (2002a) was the first of its kind in thoroughly evaluating the potential of digital photogrammetric point clouds for the determination of stand mean tree height. In this study, two adjacent stereo pairs of panchromatic digital images were processed with an automated image matching software (i.e. Match-T, version 2.2). This produced sparse point clouds (0.03 – 0.05 canopy points m^2) from which explanatory variables were extracted and then used to model mean tree height according to an area-based-approach (ABA; see section 4.1.1). The results by Næsset (2002a) showed the presence of rather large systematic errors leading to an underestimation of 5.42 m of the ground-truth stand mean height, especially for mature forests. Furthermore, Næsset (2002a) also found that the precision obtained was equal to manual photogrammetric measurements and smaller than that achieved using airborne laser scanning (ALS) data. These results did not indicate any particular advantages of the use of digital photogrammetry compared to alternative manual methods or methods using alternative RS technology. At the time, the development of photogrammetric algorithms was relatively slow and improvements in the automation of the image matching and the processing speed were critically needed (Baltsavias 1999, Næsset 2002a). During the same years, ALS data also became an attractive 3D RS data source and after encouraging results from initial case studies (Næsset 2002b, Holmgren 2004) became the main source of RS auxiliary data in state-of-the-art FMI. As a result, in the past 20 years, FMIs based on 3D RS data have relied mostly on ALS as a more effective RS data source than photogrammetric point clouds. Because of the importance of ALS data in forest inventories, this data source was used throughout this thesis as the benchmark to compare the performance of photogrammetric data.

1.3 Modern digital photogrammetry

Although ALS data have many advantages (e.g. direct measurement of height, penetration of vegetation), aerial imagery still represents an essential data source for forest inventory. Therefore, nowadays aerial imagery are acquired frequently for vast areas for orthophoto production. In several countries in Europe there are national programs devoted to the regular

acquisition (i.e., intervals of 5 – 6 years) of aerial imagery (Stepper et al. 2014a, Ginzler and Hobi 2015, Waser et al. 2015). In addition to an increased availability of imagery, the development of photogrammetric software has seen a rapid increase in the past 15 – 20 years. Since the late 2000's, advances in computer vision, image matching algorithms and increased computing power have fueled a renaissance in the use of aerial images for the generation of high-resolution 3D data using image matching (Baltsavias et al. 2008). Many photogrammetric software packages (proprietary and open-source) have been and continue to be developed, offering unparalleled possibilities to produce 3D data from any kind of overlapping imagery. Furthermore, photogrammetric data can be generated by single users on their own desktop (Baltsavias 1999).

In this thesis, modern photogrammetric data from large-format frame-cameras acquired from manned aircrafts was defined as digital aerial photogrammetry (DAP). DAP has become attractive both for research and commercial activities because of a combination of: 1) smaller acquisition costs than ALS due to the larger coverage attainable due to the higher flying altitudes and larger swath widths (Baltsavias 1999) and (2) high resolution of the point cloud (i.e. up to the size of ground sampling distance). The studies from Baltsavias et al. (2008), Waser et al. (2008), and St-Onge et al. (2008) represent the first examples of DAP applied to forest environments. During the past four years there has been increasing interest in the use of DAP to model forest biophysical properties as a cost-effective solution to airborne laser scanning (ALS) for ABA forest inventories. Initial benchmarking studies compared the performances of DAP point clouds against ALS for modeling typical forest biophysical properties of interest (Bohlin et al. 2012, Järnstedt et al. 2012, Nurminen et al. 2013, Straub et al. 2013a, Vastaranta et al. 2013, Gobakken et al. 2014, Pitt et al. 2014, Rahlf et al. 2014, Ota et al. 2015, White et al. 2015, Yu et al. 2015, Puliti et al. 2016). These studies proved that despite intrinsic differences between the data and the models used, the predictions of forest attributes using DAP models were similar to ALS based forest inventories (Figure 1). The differences in root mean square error as percentage of the mean ($RMSE_{\%}$) reported in the abovementioned studies between the two methods were limited to 0.22 – 9.62% for tree height, 0.58 – 8.41% for mean diameter, 1 – 8.34% for basal area, 1.6 – 4.5% for stem number, and 0.5 – 9.13% for GSV.

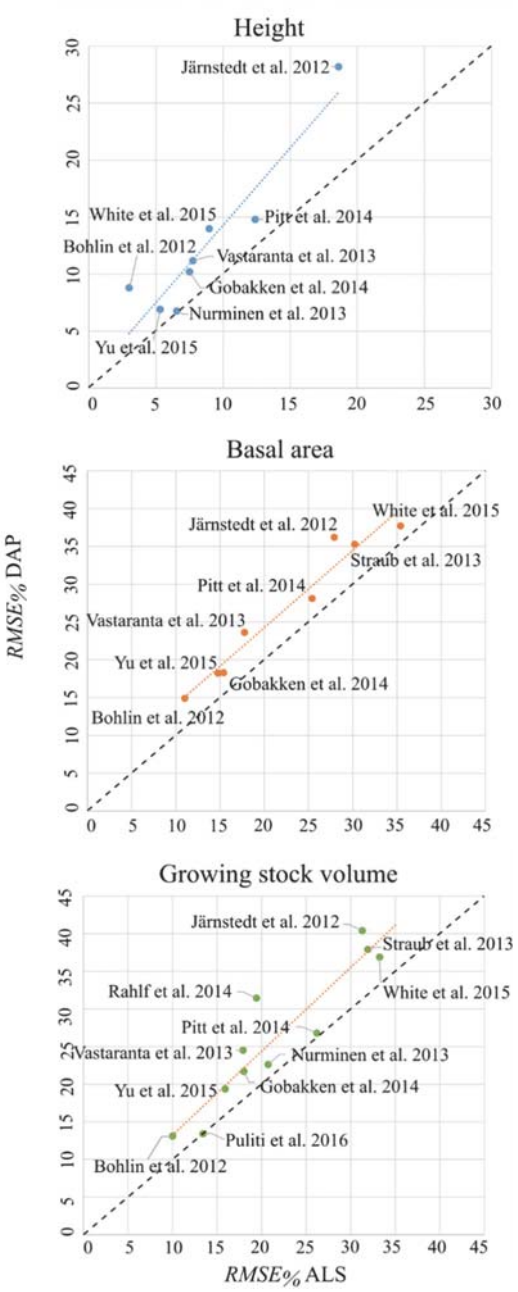

Figure 1. Scatterplots of root mean square error as percentage of ground reference mean value ($RMSE_{\%}$) obtained using ALS on the horizontal axis, and the $RMSE_{\%}$obtained using DAP on the vertical axis. The different observations illustrate the comparisons of the two data sources by different studies. The graphs represent the $RMSE_{\%}$ for height, basal area, and volume since these were some of the common forest biophysical properties to most of the studies. The 1:1 line is represented as a dark dashed line, while the trend lines for the data used are given in lighter colors.

Although most studies were carried out in boreal conifer-dominated forests, there were also some conducted in seasonal tropical forests (Ota et al. 2015), temperate broadleaf-dominated forest (Stepper et al. 2014a, Stepper et al. 2014b), and highly timbered (maximum gross volume = 2481.9 m^3 ha^{-1}) coastal temperate rainforests (White et al. 2015). Irrespective of the different forest types, the results were highly consistent, showing similar accuracies between DAP data and ALS.

The main limitation in these studies was the need for a high-resolution digital terrain model (DTM) from ALS data in order to obtain relative height above ground (i.e. normalize) from the DAP point cloud. In the only case where a DTM was generated from DAP rather than an ALS (Ota et al. 2015), the accuracy of the results worsened significantly. In some countries in Europe, ALS DTMs are increasingly available thanks to national ALS acquisition campaigns, however these data are only available in a few countries.

One important aspect that makes photogrammetry competitive with ALS data is the larger variety of platforms and sensors that can be used to acquire imagery. There are examples in the literature of forest inventories carried out using photogrammetric data generated from satellite image stereo-pairs (Hobi and Ginzler 2012, Persson et al. 2013, Straub et al. 2013b, Montesano et al. 2014, Neigh et al. 2014, Yu et al. 2015, Immitzer et al. 2016, Persson 2016), DAP (see the already mentioned studies), and unmanned aerial vehicle (UAV) imagery (see section 1.4 below).

1.4 UAV photogrammetry

In recent years, the civilian market for UAVs has increased rapidly and as a result, these RS data acquisition platforms are nowadays largely available. UAVs may be equipped with a variety of sensors, however most often consumer grade cameras have been used for acquiring imagery. Differently from the imagery used to generate DAP, UAV imagery is often characterized by large perspective distortions, poor camera geometry, lack of spectral consistency, and poor positioning accuracy. Such characteristics limited the use of such imagery for photogrammetric processing in the past. Nevertheless, since the inclusion of advanced structure from motion (SfM) algorithms in photogrammetric pipelines (Whitehead and Hugenholtz 2014), there has been a boost in the interest in UAV photogrammetry. SfM algorithms allow for the estimation of the camera's exterior parameters (i.e. position and orientation) from an unordered but overlapping series of images (Dandois and Ellis 2013). Such parameters are fundamental in order to ensure accurate photogrammetric measurements.

Because of these technological advances, photogrammetric data from UAV imagery, hereafter denoted as UAV data, have become an increasingly popular photogrammetric product. The combined effect of advances in photogrammetric software and wide availability of UAVs (Puliti et al. 2015) provides a large number of users not only with advanced photogrammetric software but also with the possibility of acquiring their own 3D RS data on demand.

Since the first studies using UAV data for forest inventory purposes (Dandois and Ellis 2010), there has been a rapid increase in the literature available on the topic (Dandois and Ellis 2013, Lisein et al. 2013, Getzin et al. 2014, Paneque-Gálvez et al. 2014, Sperlich et al. 2014, Dandois et al. 2015, Puliti et al. 2015, Tuominen et al. 2015, Zahawi et al. 2015, Kachamba et al. 2016, Wallace et al. 2016, Zhang et al. 2016, Puliti et al. in submission). UAVs have become attractive because of the flexibility they offer in data acquisition and thanks to the very high level of detail characterizing the imagery acquired at low flight altitudes (e.g. 120 m above ground). The flexibility of UAV data is demonstrated by the large variety of forest types studied, including: temperate broadleaves-dominated forests (Dandois and Ellis 2013, Lisein et al. 2013), boreal conifer-dominated forests (Puliti et al. 2015, Tuominen et al. 2015), tropical forests (Paneque-Gálvez et al. 2014, Zahawi et al. 2015), tropical woodlands (Kachamba et al. 2016), sclerophyll eucalypt forests (Wallace et al. 2016), evergreen broadleaved forest (Zhang et al. 2016). Overall, the results have demonstrated that UAV data could be used to model forest biophysical properties of interest like GSV or biomass with $RMSE_{\%}$ in the range of: 14.5% – 46.7%. Regardless of the large range in $RMSE_{\%}$, the results were comparable to what could be obtained using ALS data. This thesis further investigated the possibility to use these data in forest inventories (both FMI and LSFS).

1.5 Forest inventories based on 3D RS auxiliary

When describing forest inventories it is important to distinguish between forest management inventories (FMI), and large scale forest surveys (LSFS). Both types have in common a long history of combining sample of field plots with RS data for the assessment of forest resources (McRoberts et al. 2014a). The advantage of including RS data to samples of field plots derives from the correlation between RS data and forest biophysical properties. In this regard, 3D RS data sources have proven to be highly correlated with variables like mean height, basal area, and GSV. FMI and LSFS differ in the end-users and in the spatial scale at which

they are carried out. FMI are performed at a local level (i.e. forest property level) to support the decision making of forest managers and typically result in detailed maps (i.e. stand level) of the forest biophysical properties of interest. On the other hand, the aim of LSFS is to provide overall estimates over large areas (i.e. from municipality to national/international level) to support strategic decision making of policy makers.

1.5.1 Forest management inventories

As previously mentioned (see section 1.2), in the past 16 years FMI based on 3D RS data have become increasingly popular. The operational use of these data for FMI has proven effective in reducing the costs of forest management compared to alternative approaches (Eid et al. 2004). FMI typically rely on an area based approach (described in detail in section 4.1.1), to obtain stand level predictions. In ABA FMI large focus is on the quality of the model predictions at stand level and little work has been done to estimate the uncertainty at of the estimated stand level means (McRoberts et al. 2014a).

1.5.2 Large scale forest surveys

Differently to FMI, the objective of LSFS is to estimate a population parameter (mean or total) for a variable of interest (e.g. GSV or biomass) over a defined study area. An important part of LSFS is the estimation of the uncertainty of the population parameter (i.e. variance).

Historically, LSFS have been carried out using a probability sample of field plots in design-based inference (DB). The population parameter is estimated from the field plot information and the reliability of this estimate lies in the probabilistic nature of the sampling design. DB has the advantage of providing design-unbiased estimates; however the estimate of the population parameter can deviate from the true value especially when only a small sample size is available. In this thesis, DB inference was used to provide a reference for an LSFS approach relying only a probability sample of field plot data, i.e. no RS were available.

When RS auxiliary data are available for the entire area in addition to georeferenced field plot data, models can be developed linking the two sources of information and predictions can be made for the area covered by the RS data. In this case, the model forms the base for inference as the population parameters are estimated from the predicted values according to an ABA. The estimated variance of the population parameter derives from the uncertainty in model parameter estimates (McRoberts 2006). Thus, this inferential framework is referred to as model-based (MB). One of the main advantages is that for MB the field plots are only used for fitting a model that is suitable to the study area. Hence, the inference does not rely on the randomization in the field plots enabling the use purposive sampling or even

the use of external models. A drawback of MB is that the model parameter estimates can be biased if the model is not correctly specified. In this thesis, MB inference was used when wall-to-wall RS auxiliary data was available (i.e. ALS data and Sentinel-2 imagery).

When the acquisition of RS auxiliary data are expensive over large areas (e.g. ALS or UAV data), the costs can be reduced by acquiring only a sample of RS data. This increased complexity in the sampling design allows for an increased precision of the field based estimates while not incurring in excessive costs. Nevertheless, the increased complexity requires a rigorous reporting of the uncertainty estimates (Gregoire et al. 2016). In an effort to ensure this rigorousness, Ståhl et al. (2011) developed an inferential framework based on a two-phase design. In the first-phase a probability sample of RS data are acquired and in the second-phase a subsample of field data are acquired. Similarly to MB, a model linking field plot information and RS auxiliary is developed and applied to the first phase sample and the predictions used to estimate the population parameter. The uncertainty of the estimates in this case derives both from the uncertainty of the model parameter estimates and from the sampling error related to the sample of RS data (first-phase sample). As this inferential framework draws from both DB and MB, it is often referred to as hybrid (HYB) inference. This method has proven to be effective in increasing the precision compared to pure field based estimates (Ene et al. 2012, Ene et al. 2013, Ene et al. 2016) while not incurring excessive costs for extensive RS data acquisition. HYB inference similarly to MB has the advantage of being rather flexible in terms of not requiring a probability sample of field plots, enabling both the estimation in inaccessible areas (McRoberts et al. 2014b) as well as the use of purposive sampling designs. In this thesis, HYB inference was adopted using a sample of field plots and UAV data as a means to reduce the costs of UAV data acquisition for forest inventories.

The recent increase in the availability of RS data has inspired researchers to combine multiple RS data sources as means to further increase the precision and the extent of LSFS and therefore their cost-efficiency. One of the most interesting applications has been the use of multiresolution approaches linking field plots, a sample of high resolution 3D RS auxiliary (e.g. ALS) and global coverage space-borne information. The different levels of information are characterized by an increase in resolution, quality of the information, and acquisition costs when going from space-borne to field data. These type of LSFS have been object of study since the late 2000's (Boudreau et al. 2008, Nelson et al. 2009, Andersen et al. 2012, Neigh et al. 2013, Strunk et al. 2014, Margolis et al. 2015, Nelson et al. 2016). The

assessment of the benefits from these types of LSFS has been difficult because of the lack of statistically rigorous variance estimators accounting for the uncertainty of the different models involved in the estimation. Groundbreaking research from Saarela et al. (2016) aimed at developing an inferential framework for this type of LSFS. In their work, Saarela et al. (2016) used three levels of information: (1) field plots, (2) a sample of ALS data, and (3) wall-to-wall Landsat data. The different levels of information were linked through nested models, upscaling ground reference GSV to the sample of ALS data and then to the entire study area using Landsat data. The novelty of the hierarchical model-based inference (HMB) lies in the variance estimator, which accounts for the uncertainty of each of the models' parameters. This thorough reporting allows for a clear picture of the precision of these estimators when compared to MB or HYB estimators. An advantage of this method is that being in the realm of MB inference, both the field plots and the sample of RS auxiliary can be collected according to purposive or opportunistic criteria. In this thesis, HMB inference was used when combining a sample of field plots, with partial-coverage UAV data, and with wall-to-wall Sentinel-2 data.

2. Objectives

The objective of this thesis was to investigate the potential of using digital photogrammetry for FMI and for LSFS. The specific objectives were to:

1) quantify the accuracy of FMI when using structural and spectral information obtained from photogrammetric data acquired with different image acquisition platforms (Paper I and II);
2) identify operational niches for UAV data in LSFS by using it as part of a sampling strategy (paper III and IV).

The papers included in the thesis are:

I. *Assessing 3D point clouds from aerial photographs for species-specific forest inventories* – Explores the possibility to use structural and spectral variables from DAP for species-specific FMI. The DAP data was generated from UltraCamXP imagery collected from a manned aircraft.

II. *Inventory of small forest areas using an unmanned aerial system* – Illustrates one of the first examples where a UAV was used for acquisition of high resolution photogrammetric data for small scale (2 km^2) FMI. Structural and spectral variables were used to model forest biophysical properties like Lorey's height, dominant height, basal area, number of trees, and GSV.

III. *Use of partial-coverage UAV data in sampling for large scale forest inventories* – Shifts the focus from the use of UAV data for FMI to using them as part of a sampling strategy in LSFS. UAV data were acquired as a sample (UAV blocks) over a large area (130 km^2) and together with a sample of field plots were used to estimate mean GSV and its uncertainty for the entire area in a hybrid inferential framework.

IV. *Combining UAV and Sentinel-2 auxiliary data for forest growing stock volume prediction through hierarchical model-based inference* – Builds upon the sampling approach adopted in paper *III* by adding a wall-to-wall layer Sentinel-2 multispectral data. Hierarchical model-based inference was adopted for the estimation of the uncertainty of all of the models linking the three levels of information (i.e., field plots, UAV, and Serntinel-2 data).

3. Materials

3.1 Study areas

Three study areas located in southeastern Norway (see Figure 2) were used in the thesis:

a) A boreal forest area in Våler municipality (8.5 km^2) was used in paper I. The forest area is dominated by conifer species, with Norway spruce (*Picea abies* (L.) Karst.) being the dominant species (51% of the GSV) followed by Scots pine (*Pinus sylvestris* L.) and a small portion of deciduous species (13%). The area is characterized by a rather flat terrain with the altitude ranging between 70 and 120 m above sea level. The forests have been actively managed and the area has been subject to repeated ALS assisted FMI (Næsset 2002b, Gobakken et al. 2014);

b) A subset of the study area at Våler (1.9 km^2) was used in paper II. The area was selected as it represented an example of private forest property in Norway.

c) A forest area in Gran municipality (131 km^2) was used in paper III and IV. The area was selected as a subset of a larger operational FMI ongoing in the district. As in the Våler study area, the dominant species was also Norway spruce (*Picea abies* (L.) Karst.), followed by Scots pine (*Pinus sylvestris* L.), and deciduous species. The topography was more hilly than in Våler and the altitude varied between 130 to 560 m above sea level.

For all of the above sites, the forests of interest had a mean height > 7 m as the forest in this development stage are typically inventoried by means of RS in FMI in Norway (Puliti et al. in submission).

3.2 Field data

For each study area, field measurements were collected during the same vegetative season as the RS data acquisition. For all studies, a systematic sampling design was adopted for the selection of the location of the field plots. This allowed for a uniform distribution of the plots throughout the study areas while also ensuring a probability sample. For study area *a*, two different sets of field plots were acquired: a sample plot dataset including 151 circular field plots (400 m^2), and a stand validation dataset composed of 63 stands within which 744 field plots (125 – 250 m^2) were distributed systematically ensuring an average coverage of 37.3% of the stand area. For study area *b*, a subset of 38 plots from the sample plot dataset used in *a* were chosen. For study area *c*, 33 field plots (500 m^2) were acquired in two different sets of plots. The first included 26 field plots within the study area and the second included seven field plots collected as part of a larger inventory in a contiguous area. Figure 2 illustrates the sampling designs adopted in his thesis for the different study areas.

For all of the field plots, diameter at breast height, i.e. 1.3 m above ground (DBH) was measured for all trees with DBH ≥ 4 cm. Heights were measured for a sample of trees selected based on probability proportional to stem basal area. The position of the center of each plot was recorded with sub-meter accuracy using differential global positioning systems and global navigation satellite systems. Forest biophysical properties were directly computed from the DBH and height measurements. These included Lorey's height (h_L), dominant height (h_{dom}), number of trees (N), and basal area (G). GSV values were obtained using the DBH and height measurements with the allometric equations from Braastad (1966), Brantseg (1967), and Vestjordet (1967), Vestjordet (1968), Fitje and Vestjordet (1977).

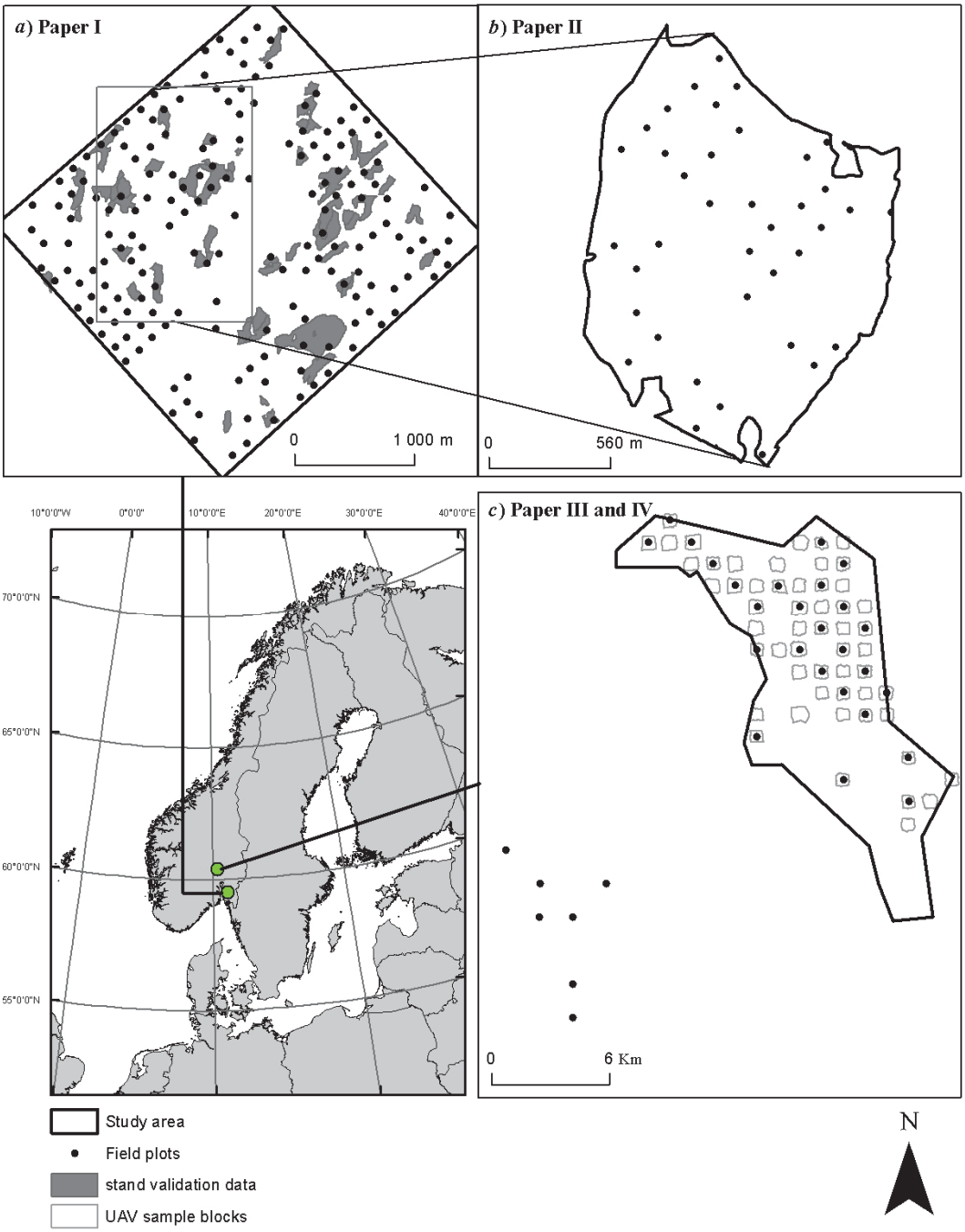

Figure 2. Overview of the location and field sampling designs adopted in this thesis. Study area *b* (paper II) was a subset of *a* (paper I).

3.3 Remotely sensed data

Different RS data sources were used for each study area. These differed in the type of sensor used (active and passive sensors), data acquisition platforms (satellites, manned aircrafts, and UAVs), and coverage (wall-to-wall and partial-coverage). A summary with the technical specifications of all the remote sensing datasets used in this thesis is provided in Table 1.

3.3.1 ALS data

For all of the study areas, wall-to-wall ALS data were acquired using fixed-wing manned aircrafts. These consisted of two dataset: 1) in study areas *a* and *b* ALS data were acquired using an Optech ALTM-Gemini laser scanner and resulted in an average pulse density of 7.45 points m^{-2}; 2) in study area *c* the ALS data were acquired using two Leica ALS70 and also had an average point density of 7.45 points m^{-2}.

In this thesis, ALS data were used as a benchmark data source for forest inventories to compare the results obtained with photogrammetric data. Also, in all of the studies, the ALS derived DTMs were used to normalize the photogrammetric point clouds.

3.3.2 Digital aerial photogrammetry

The same aircraft used for acquisition of ALS data in study area *a*, was used to acquire wall-to-wall aerial imagery using Vexcel UltraCamXP. This is a large-format digital aerial frame-camera. The flight altitude was 2850 m above ground and the acquisition of two flight strips lasted for approximately 7 minutes. The ground sampling distance (GSD) of 0.17 m for the panchromatic images and 0.51 m for the multispectral bands (i.e., red, green, blue, near infra-red). The images were captured with a forward and lateral overlap of 80% and 30%, respectively.

Photogrammetric processing was performed using Agisoft Photoscan (Agisoft 2014). The data vendor provided internal and external orientation parameters. The resulting point clouds were "colorized" by co-registering them with the unrectified imagery using the interior/exterior camera parameters and *x*, *y*, *z* coordinates of each point. The photogrammetric processing also produced a panchromatic orthophoto at 17 cm resolution.

3.3.3 UAV data

UAV data was collected in study areas *b* and *c* using a fixed wing senseFly eBee UAV (senseFly 2014). The fixed wing solution was adopted in this thesis as it enabled larger area coverage compared to multirotors. For study area *b*, the acquisition was done on several contiguous flights ensuring wall-to-wall coverage, while for area *c*, UAV data was acquire only as partial-coverage on 55 systematically distributed blocks of 41.1 ha on average.

Two different consumer-grade cameras were used for this thesis: Canon S110 near infra-red (NIR) camera (in study area *b*) and a Canon IXUS/ELPH camera (in study area *c*). The NIR camera produced a three bands image representing the red, green, and near infra-red bands, while the second camera registered only the RGB bands. The resolution for the NIR

camera was lower (12 MP) than the RGB one (16 MP) while the focal length was the same for both sensors (i.e. 24 mm). For both acquisitions, the overlap was set to 90% forward overlap and 80% later overlap. However, as explained in Puliti et al. 2015 this did not correspond to the actual overlap because of limitations in the UAV used. In addition, perpendicular flight lines were also flown. In a preliminary testing phase, this image redundancy was found to be necessary to reduce the occlusions and generate a uniform 3D geometry through photogrammetric processing in forested environments. National aviation regulations limited the acquisition of UAV imagery in altitude (i.e. maximum of 120 m above ground) and horizontally (i.e. visibility of the UAV at all times). This resulted in the need for conducting 15 flights in area *b* and 55 flights for study area *c*.

Photogrammetric processing was performed using Agisoft Photoscan (Agisoft 2014) as it was found to be a versatile and user friendly software for generating 3D point clouds from UAV imagery. A minimum of five ground control points (GCPs) were always used for correcting shifts and distortions due to the poor geolocation and inertial measurement information from the UAV. The resulting dense point clouds (i.e., 60 – 90 points m^2) were normalized using the available ALS DTM.

A visual comparison between DAP data acquired from a manned aircraft and UAV data used in this thesis is shown in Figure 3.

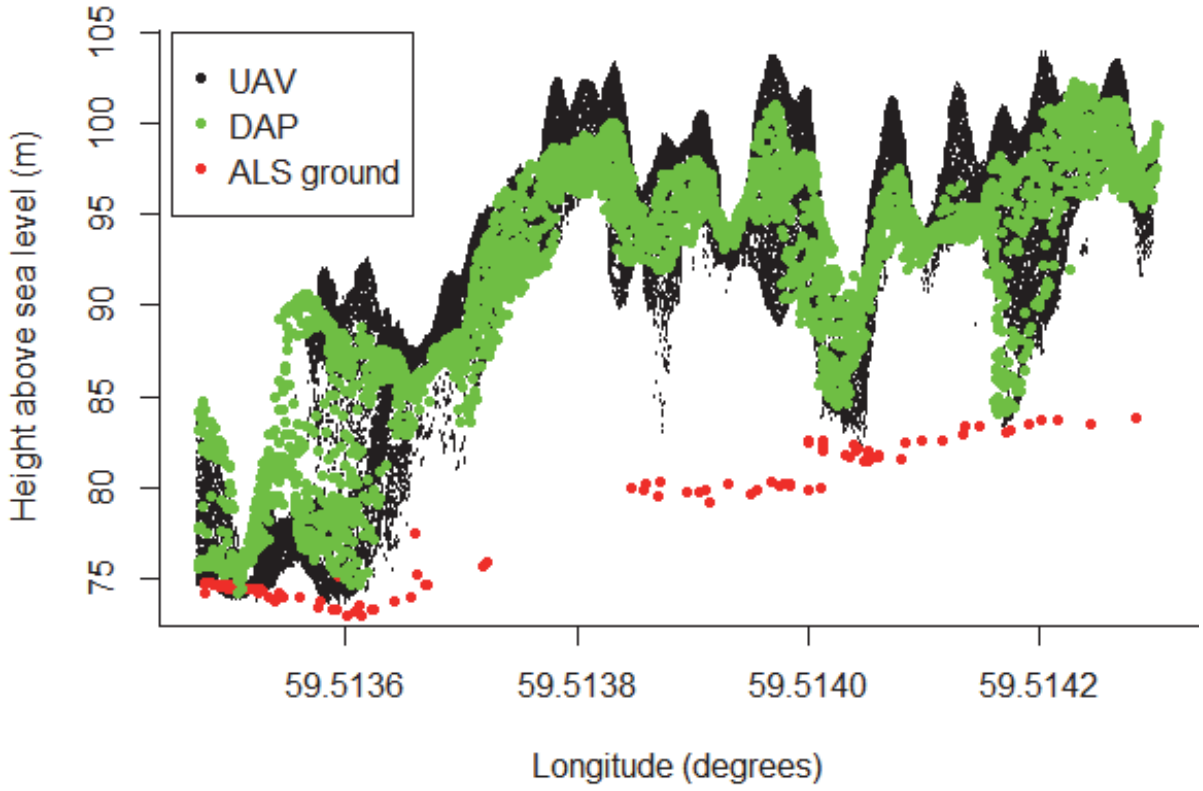

Figure 3. Visual comparison of UAV data (black dots), DAP acquired from a manned aircraft (green dots), and ground ALS returns (red dots) for a transect using the three data sources in area *b*. The UAV data were collected in November 2014, while DAP data were acquired in July 2010.

3.3.4 Sentinel-2 data

For the purpose of paper IV, Sentinel-2 multispectral imagery were acquired using the Multi Spectral Instrument (MSI) during August 2015 for study area *c*. The MSI is a push-broom sensor. The entire area was covered by two overlapping Sentinel-2 level 1-C tiles. Level 1-C top-of-atmosphere reflectance were processed into level 2-A bottom-of-atmosphere products using software provided by the European Space Agency (ESA).

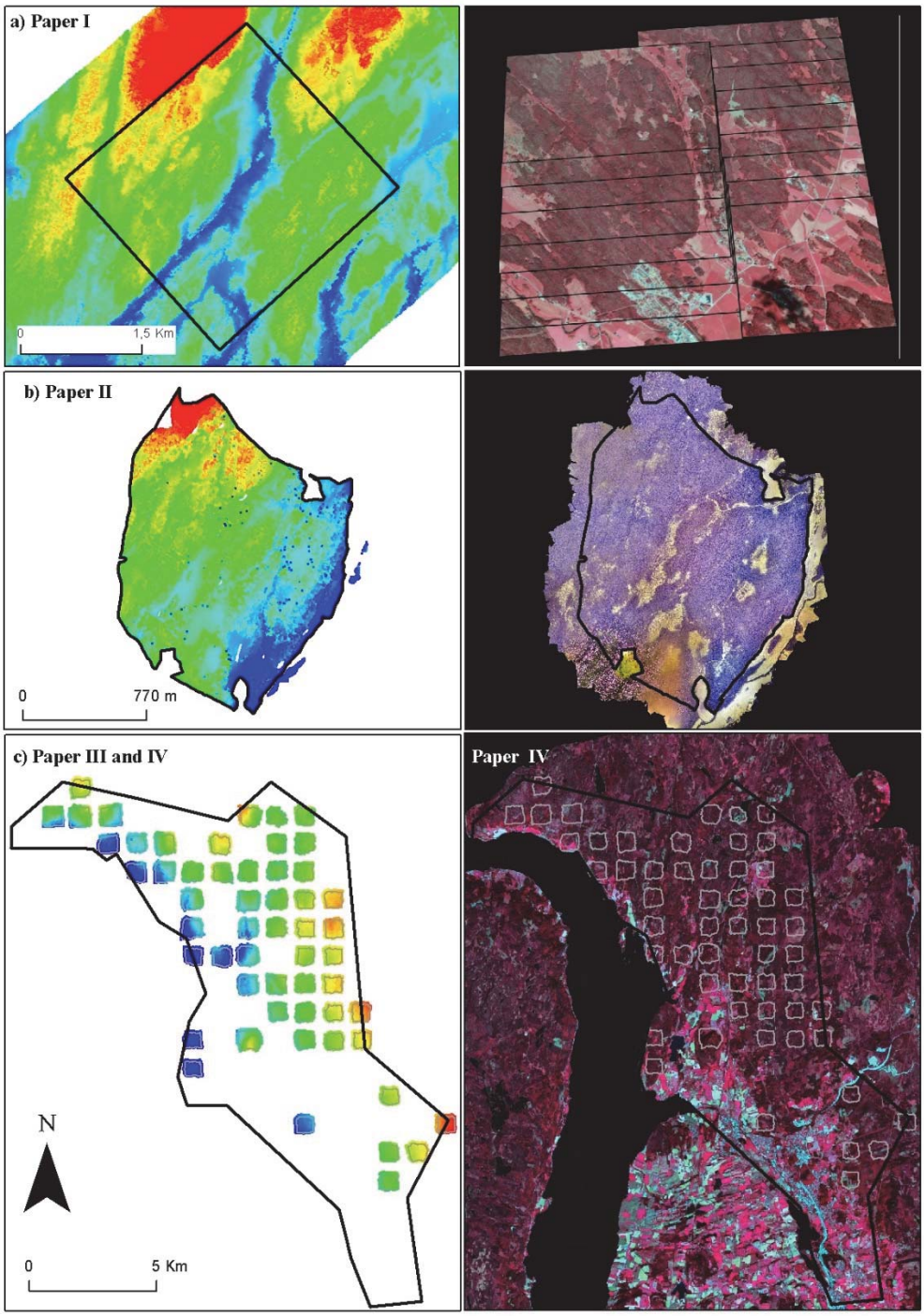

Figure 4. Overview of the photogrammetric (on the left column) and image datasets (on the right column) used in this thesis. In the left column the colors represent the altitude above sea level (i.e., higher altitudes with warmer colors) for the photogrammetric point clouds derived from: UltraCamXP imagery (study area *a*, paper I), UAV imagery using the NIR camera (study area *b*, paper II), and UAV imagery using the RGB camera (study area *c*; paper III and IV). In the right column the multispectral data used in the thesis are shown: RGB-

NIR unrectified imagery from UltraCamXP (paper I), RG-NIR orthophoto from UAV (paper II), and Sentinel-2 imagery displayed in false color (paper IV).

Table 1. Summary of the technical specifications for all the RS datasets used in the different study areas (*a*, *b*, and *c*).

Study area	Technical specifications					
	a		*b*	*c*		
Platform	Manned Aircraft		UAV	Manned aircraft	UAV	Satellite
Sensor	Optech ALTM-Gemini	UltraCam XP	Canon S110 NIR	Leica ALS70	Canon IXUS/ ELPH	MSI
Altitude above ground (m)	900	2850	120		120	786 Km
Side overlap	-	30	80	-	80	-
Forward overlap	-	80	90	-	90	-
Ground sampling distance	7.4 points m^{-2}	Pan: 17 cm RGBI: 51 cm	4 cm	7.4 points m^{-2}	4 cm	10 - 30 m

4. Methods

4.1 Common methods to all papers

4.1.1 Area based approach

In all the studies included in this thesis, an area based approach (ABA) was adopted for combining the RS with field data. The ABA relies on the area-based relationship between RS information and ground reference forest biophysical properties (Vauhkonen et al. 2014). In this thesis the RS data were clipped from the area covered by the field measurements (i.e., area of the field plot). These predictor variables were then used to fit models at plot level against ground reference forest biophysical properties. With the exception of paper II, these models were then applied to predict the forest biophysical properties on the entire auxiliary space. Prior to applying the model, the study areas were tessellated into grid cells with equal size corresponding to the size of the field plots. RS predictor variables were extracted for each grid cell. The grid cell predictions were then averaged at stand level when stand boundaries were available (paper I), or used as the basis for the estimation in LSFS (paper III and IV).

4.1.2 Modelling

For all of the studies included in the thesis, multiple linear regression models were used to link field observations to RS predictor variables. The choice to use these models was driven by the fact that: 1) they enable a clear reporting of the variance covariance matrices, 2) they can be used when only small samples of field plots are available. Other than in paper IV, transformations of the variables were performed as these have been found to this has previously been shown to be suitable for the modeling of these properties (Næsset 2002b). In paper IV, no transformations were applied to ensure a comparison with some of the methods presented in this paper which only allowed for linear models.

For all of the studies, a maximum of five predictor variables were selected automatically using a branch-and-bound search for the best subset (i.e., R-package *leaps*; Lumley and Miller (2009)). The Bayesian information criterion was used for model selection. Furthermore, the variance inflation factor was used to account for multicollinearity. The subset with one variable less was iteratively selected if any of the variables in the current subset had a variance inflation factor ≥5.

In addition to multiple linear regression models, Dirichlet regression (i.e. R-package *DirichletReg*; Maier (2014)) was used to model tree species proportions by means of spectral variables in paper I. The Dirichlet regression is similar to the beta-regression with the advantage that it allows for simultaneously modelling of all of the species proportions.

4.1.3 Structural variables

Structural variables were extracted for each plot and grid cell from the photogrammetric and ALS point clouds. These included height and density variables: height percentiles (p_{10}, p_{20},…, p_{95}, p_{100}), density metrics (d_0, d_1,…, d_9), and standard deviation (h_{sd}). In paper I these were used to model species proportions (in addition to spectral variables, see section 4.1.4), and GSV. In paper II, in addition to GSV, structural variables from UAV data were used to model additional forest biophysical properties, i.e. Lorey's height (H_L), dominant height (H_{dom}), stem number (N_{ha}), basal area (G_{ha}). In paper III and IV, the same height and density metrics were used to develop GSV models using ALS data or UAV data.

4.1.4 Spectral variables

Spectral variables were also used in paper I, II, and IV. These were derived at plot and grid cell level either from the digital number value of pixels or directly from the "colorized" point clouds. The spectral variables were subdivided into tonal and textural variables. The following tonal variables were used in paper I, II, and IV: mean band values, standard

deviations, and band ratios. Textural variables (Haralick et al. 1973) extracted at pixel level from the panchromatic orthophoto were also tested in paper I.

The spectral variables were used in paper I for modelling species-proportions using Dirichlet regression, while in paper II tonal variables were used in addition to structural variables in the modelling of H_L, H_{dom}, N_{ha}, G_{ha}, and GSV. In paper II, to better understand the benefit of using the spectral information, models including spectral and structural variables were compared to models using only structural variables. In paper IV, tonal variables extracted from coarse resolution Sentinel-2 imagery were used to model GSV.

4.2 Accuracy assessment FMI

The accuracy of FMI based on photogrammetric data was assessed for data generated from imagery captured using different sensors (i.e., large-format frame-cameras and consumer-grade cameras) and acquisition platforms (manned aircrafts and UAVs). In paper I and II, the performance of DAP and UAV data was assessed based on the accuracies of the GSV models. In paper I, the accuracy assessment was done for the following response variables: species proportions, dominant species classification, and species-specific GSV. In paper II, additional biophysical properties were assessed, i.e. H_L, H_{dom}, N_{ha}, and G_{ha}. The models were evaluated in terms of: adjusted R^2 (R_a^2), root mean square error ($RMSE$), $RMSE$ as percentage of the mean ($RMSE_{\%}$), mean difference ($\overline{D}$), and $\overline{D}$ as percentage of the mean ($\overline{D}_{\%}$). For the dominant species classification (paper I) a confusion matrix was used to evaluate commission, omission, and overall errors. For both studies, these values were calculated at plot level using leave-one-out cross validation. Furthermore, in paper I the accuracy assessment was also carried out at stand level using the available independent data (see section 3.2). In paper I, the results obtained using ALS were used as reference to evaluate the performance of DAP.

4.3 Use of UAVs as a sampling tool for LSFS

After assessing the accuracy of FMI using UAV data for modelling GSV in paper II, the focus of the thesis shifted towards defining cost-efficient applications for the use of UAV data in forest inventories (paper III and IV). One possible way to reduce the costs is to use UAV data as part of a sampling strategy to estimate GSV in LSFS. Hence, paper III introduced an inventory approach where a sample of field data and a sample of UAV data were used in a HYB inferential framework for the estimation of GSV for a study area of approximately 70 km^2 (denoted as case B). Paper IV, building upon paper III attempted to further increase the

precision of the estimation by including an additional wall-to-wall layer of Sentinel-2 imagery (denoted as case C). In paper IV the HMB estimator developed by Saarela et al. (2016) was adopted.

The proposed cases B and C were compared against the following alternative inventory cases that differed in terms of sampling designs, mode of inference, and source of auxiliary data:

Case A.1: Standard model-based inference with wall-to-wall ALS data (paper III and IV). This case represented the best-case scenario in terms of the quality of the auxiliary data and auxiliary data coverage.

Case A.2: Standard model-based inference with wall-to-wall Sentinel-2 data (paper IV). This case was used to gain insights on the attainable precision using field plot and Sentinel-2 data alone for estimation of GSV.

Case B: Hybrid inference with a sample of UAV data (paper III and IV). See description above.

Case C: Hierarchical model-based inference with wall-to-wall Sentinel-2 and a sample of UAV data (paper IV). See description above.

Case D: Design-based inference with a probability sample of field plot data (paper III). This case was the only one where no remote sensing data was available.

The relative efficiency (RE), calculated as the estimated variance of one case divided by the estimated variance for another case, was used as a measure of improvement of precision of one case over another. Furthermore, as the main reason to use UAVs in a sampling context was to increase the cost-efficiency of UAV forest inventories, cost figures were reported and discussed. A graphical summary of the different field and RS auxiliaries used in the different cases is provided in Figure 5.

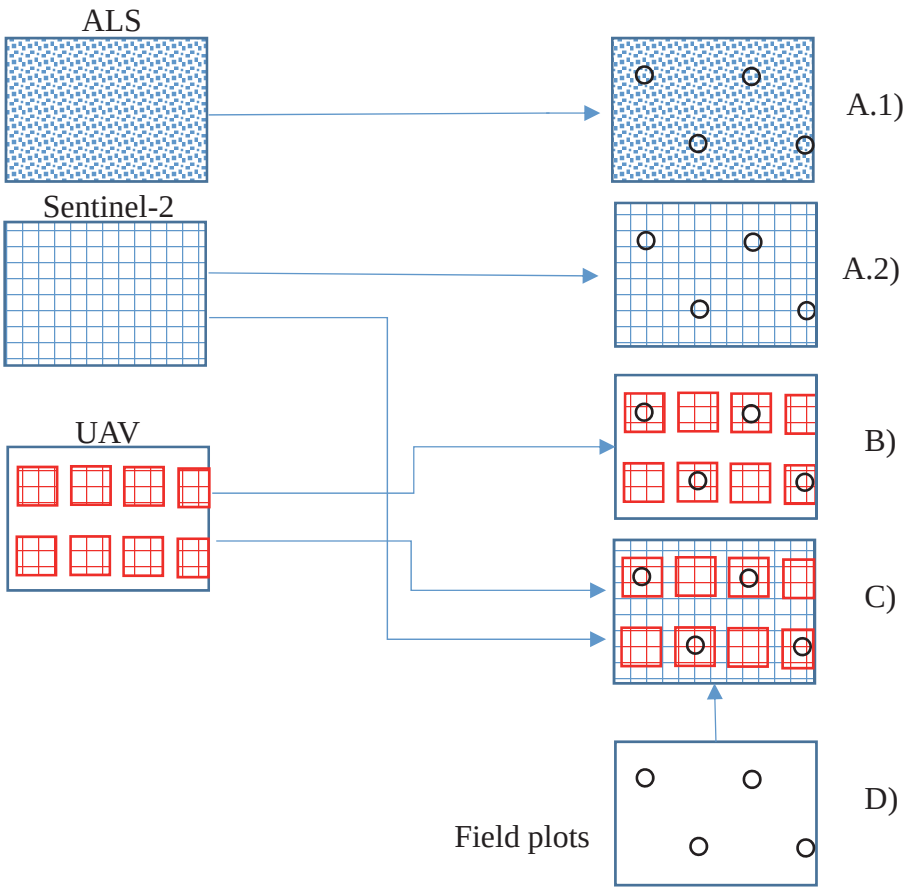

Figure 5. Schematic representation of the LSFS cases object of study.

4.3.1 Hybrid inference

Case B was adopted both in paper III and IV. In the former, it was used as a means to improve the precision of field DB estimates, while, in paper IV the precision of case B was used as reference for quantifying the improvement in precision when adopting case C. Case B relied on a two-phase design, where UAV data were acquired in the first-phase as a probability sample (i.e. 55 blocks) and a sample of field data (n= 26) were acquired in the second-phase as a subsample of the UAV data. Additionally, a set of field plots (n= 7) external to the area of interest where UAV data was also available. A model linking UAV data and ground reference GSV was fitted using the entire set of observations (n= 33). The models were then applied to the previously tessellated sample of UAV data and the grid cell prediction were used to estimate the expected value $\widehat{E(\mu)}_B$ (see equations 6 and 7 in paper III and IV, respectively). The variance of the population parameter $V\left[\widehat{E(\mu)}_B\right]$ was estimated using the hybrid estimator by Ståhl et al. (2011) accounting for both the sampling error from the first phase sample and for the model error due to the uncertainty of the parameter

estimates (see equations 7 and 8 in paper III and IV, respectively). The estimated standard error ($\widehat{SE}$), calculated as the square root of the estimated variance $\hat{V}\left[\widehat{E(\mu)}_B\right]$, and $\widehat{SE}$ as percentage of $\widehat{E(\mu)}_B$ ($\widehat{SE}_{\%}$), were used as measures of precision.

Furthermore, in paper III one of the objectives was to test the possibility to improve the precision of the estimates in a hybrid inferential framework by augmenting the field data with observations external to the study area. This was addressed by comparing precision of the estimation obtained using the entire set of field plots (*n*= 33) against those obtained using only the field observation from the study area (*n*= 26).

4.3.2 Hierarchical model-based inference

Case C was adopted in paper IV as a means of further improving the precision compared to case B and to produce wall-to-wall GSV maps. In case C, three sources of information were used, namely: a sample of field plots (*n*= 33), a sample of UAV data (55 UAV blocks), and wall to-wall Sentinel-2 data. Because of the wall-to-wall coverage of the Sentinel-2 data, case C was independent from any design assumptions. The three sources of information were linked though nested models. A first model linking ground reference GSV and UAV data (GSV~UAV) was developed and applied to the UAV grid cells. Furthermore, a second model linking the grid cells predictions $\widehat{GSV}$ to the Sentinel-2 predictor variables ($\widehat{GSV}$~Sentinel-2) was developed and applied to the entire study area. These wall-to-wall grid cell predictions were used to estimate the expected value $\widehat{E(\mu)}_C$ (see equation 12 paper IV). The variance of the population parameter ($\hat{V}\left[\widehat{E(\mu)}_C\right]$) was estimated with the HMB estimator by Saarela et al. (2016). This estimator accounted for the model error due to the uncertainty of the parameter estimates for the GSV~UAV and $\widehat{GSV}$~Sentinel-2 models (see equation 13 paper IV). As for case B, the $\widehat{SE}$ and $\widehat{SE}_{\%}$ were used as measures of precision.

Furthermore, paper IV investigated the possibility of reducing the sampling intensity for the UAV data without reducing the precision of the estimates. This was addressed by simulating an iterative reduction of the UAV samples and by comparing the estimated variance in case B and in case C.

5. Results and discussion

5.1 Quantifying the accuracy of FMI when using structural and spectral information obtained with image-matching data generated from different image acquisition platforms (Paper I and II).

Consistent with previous studies comparing the performances of DAP against ALS data, the results from paper I revealed comparable accuracies when modelling GSV using ALS or DAP data (Table 2) both at plot and stand level. Among the studies mentioned in section 1.3, our findings from paper I showed the smallest differences in $RMSE$ and $RMSE_{\%}$ (i.e., 0.2 m^3 ha^{-1}; 0.1%) between DAP and ALS models (see Figure 1, growing stock volume). Similar results were also obtained when using UAV data in paper II. The $RMSE_{\%}$ obtained for models linking UAV data with Lorey's height, dominant height, stem number, basal area, and GSV were of similar magnitude of what was found by Gobakken et al. (2014) using ALS data in study area *a* (see Figure 2). In terms of $RMSE_{\%}$ for the Lorey's height, basal area, and GSV models, the results of paper II (13.6%, 15.4%, and 14.9%) were similar to those found by Tuominen et al. (2015) also in boreal forests (14.4%, 23.9%, and 26.1). Furthermore, paper II reveled larger accuracy compared to other studies using UAV data to model above ground biomass across different forest types. The larger $RMSE_{\%}$ values found by Kachamba et al. (2016) in tropical woodlands (46.7%) indicate that, as often found for ALS data, the accuracy of UAV models decreases in forests with more complex structure. Regarding the models developed using DAP or UAV data one interesting aspect was that both models included the 80^{th} height percentile, however only the UAV model included a density variable. The inclusion of a density variable in the UAV model was consistent in paper III and IV. A plausible explanation for the difference in selected variables between DAP and UAV models can be found in the larger variations in heights in the UAV point clouds compared to DAP (see Figure 3). The large overlaps used to acquire UAV data reduced the occlusions and therefore enabled a more continuous representation of the vertical distribution of the canopy. These findings confirm what was previously pointed out by Bohlin et al. (2012) and Nurminen et al. (2013), namely that increasing the image overlap results in larger height variations in the point cloud, and thus in a better representation of the vertical structure of the canopy. Furthermore, for UAV data it is also possible that the very high resolution and close range imagery enable a better detection of image features in shadowed areas and therefore a better 3D reconstruction within canopy gaps.

Table 2. Summary of accuracy assessment for the models used in paper I and II using ALS, DAP, or UAV RS auxiliary data at plot (leave one out cross validation) and stand level. The accuracy assessment included adjusted R_a^2, $RMSE$, $RMSE_{\%}$, $\overline{D}$, and $\overline{D}_{\%}$ for the GSV models for paper I and II.

				Plot level LOOCV				Stand level			
Paper	**RS data**	**Predictor variables**	R_a^2	$RMSE$	$RMSE_{\%}$	$\overline{D}$	$\overline{D}_{\%}$	$RMSE$	$RMSE_{\%}$	$\overline{D}$	$\overline{D}_{\%}$
I [a]	ALS	p_{95}, d_{50}	0.86	48.9	19.7	0.0	0.0	31.0	13.3	9.9	4.2
	DAP	p_{10}, p_{80}	0.83	49.9	20.1	0.0	0.0	31.2	13.4	-0.9	-0.4
II [b]	UAV	p_{80}, d_0	0.85	38.3	14.9	0.5	0.2	-	-	-	-

[a] the models were fitted using 151 field plots
[b] the models were fitted using 38 plots

As expected, the structural variables were strong predictors for H_L, H_{dom}, G_{ha}, and GSV. In the best case in paper II, UAV structural variables were able to describe 96% of the variation of H_{dom} and $RMSE$ was as low as 0.7 m ($RMSE_{\%}$= 3.6%). The inclusion of spectral variables improved some of the models only marginally in paper II. These findings were not surprising, as the structural variables are often able to explain most of the variability of forest biophysical properties. However, these results are far from being conclusive as the UAV imagery used were severely affected by varying illumination and atmospheric conditions. Additionally, the season (i.e., late fall, beginning of winter), the camera used, and the use of JPEG images were also sub-optimal. While UAV spectral variables were not found to be particularly relevant in paper II, in paper I, the spectral variables in combination with structural variables were useful in predicting species proportions, species-specific GSV and classifying dominant species. The maximum $RMSE$ value found in paper I for species proportions (21.4%) was in line with the study by Ørka et al. (2013) who reported a maximum $RMSE$ of 25% when predicting species proportion using a combination of ALS data and multispectral imagery. Furthermore, the overall stand level classification accuracy of the dominant species in terms of GSV was of a similar magnitude (79.0%) of that found for currently operational manual photointerpretation methods (82.5%; Maltamo et al. 2014). As in previous species-specific studies (Packalén and Maltamo 2007), large errors were observed for GSV prediction of the deciduous class (i.e., $RMSE_{\%}$= 84.9%). Despite the low accuracy for the deciduous species, the findings were encouraging for the conifer species, which were the most representative in terms of GSV, contributing to 88% of the total stand level GSV. It is worth mentioning that our results may be overly optimistic as compared to what one may expect under conditions encountered in operational applications as the imagery used in paper I were collected under constant light and atmospheric conditions.

Overall, this thesis proved that photogrammetric data acquired using different platforms and different acquisition specifications can be used similarly to ALS in FMI when an ALS DTM is available. This thesis highlighted some of the strengths of photogrammetric data like the availability of structural and spectral information from the same acquisition. The spectral data were proven to be useful to discriminate between different tree species. This thesis also provided some of the first empirical results of the use of UAV data to model a variety of forest biophysical properties. Several other positive aspects of using UAVs were pointed out in paper II, including:

1) availability of the platforms and sensors

2) versatility both in planning and in data acquisition

3) rapidity of data delivery

4) cloud insensitivity.

The results were encouraging for further use of UAVs and for this reason, this thesis further explored LSFS applications using UAVs.

5.2 Identifying operational niches for UAV data in LSFS by using it as part of a sampling strategy (paper III and IV).

The results from paper III revealed that for study area *c*, when adopting case B it was possible to increase the precision of the estimation compared to case D without incurring in prohibitive costs for wall-to-wall UAV data acquisition (see Table 3). The $\widehat{SE}$ and $\widehat{SE}_{\%}$ were reduced by 8.8 m^3 ha^{-1} and 3.8%, respectively, when case B was adopted rather than case D. The relative efficiency (i.e., $\hat{V}\left[\widehat{E(\mu)}_D\right]/\hat{V}\left[\widehat{E(\mu)}_B\right]$) was 4.4, meaning that in order to attain the same level of precision of case B but using only field plot data in a DB framework, more than four times the number of field plots would be needed (i.e. 114 field plots). In both paper III and IV the levels of precision of the estimation for case B ($\widehat{SE}_{\%}$= 3.5) were similar to what was obtained in case A.1 using wall-to-wall ALS data ($\widehat{SE}_{\%}$= 2.6). Such findings support the hypothesis that UAVs can indeed be effective as sampling tools in LSFS. Up to date, no study has addressed the use of UAV data as part of a sampling strategy for LSFS, hence no comparison was available. The estimated precision for case A.1 was consistent with what found for a similar case by McRoberts et al. (2013, 2014b) who reported $\widehat{SE}_{\%}$values ranging from 4.3% and 5.3% of the mean. The comparison for case B was limited because studies

adopting two-phase designs with ALS data rather than UAV data were carried on a much larger scale and with larger samples. Nevertheless, the increase in precision when adopting case B rather than D was in agreement with findings by Ene et al. (2012, 2013, 2016), who demontrated though simulaitions that the use of ALS data in two-phase designs under the HYB framework can be effective in increasing the precision of DB estimates.

When including a layer of wall-to-wall optical multispectral data at moderate resolution (10 – 30 m) in the estimation, as in case C, the increase in precision compared to case B was only marginal (0.32 m^3 ha^{-1}). This result was in line with the small difference in the precision ($\widehat{SE}$) found by (Saarela et al. 2016) between two cases corresponding to cases B and C in this thesis (0.3 – 0.06 m^3 ha^{-1}).

Table 3. Summary of the results from the estimation of GSV under the different cases studied in the thesis.

Case	$\widehat{E(\mu)}$	$V\left[\widehat{E(\mu)}\right]$	$\widehat{\mathrm{SE}}$	$\widehat{\mathrm{SE}}_{\%}$
A.1 [a]	250.3	37.1	6.1	2.6
A.2 [b]	209.3	171.8	13.1	5.6
B [a]	223.0	65.2	8.1	3.5
C [b]	219.6	60.2	7.7	3.4
D [a]	241.2	275.5	16.6	7.3

[a] results from paper III.
[b] results from paper IV.

Further analysis addressing the possibility to reduce the sample size of UAV data when including wall-to-wall auxiliary data revealed an increase both for $\hat{V}\left[\widehat{E(\mu)_B}\right]$ and $\hat{V}\left[\widehat{E(\mu)_C}\right]$ when reducing the number of UAV blocks (see Figure 6). Interestingly, the precision obtained with case C and using only five UAV blocks, was on the same order of magnitude ($\widehat{SE}$= 8.0 m^3 ha^{-1}) as case B using 55 UAV blocks ($\widehat{SE}$= 8.4 m^3 ha^{-1}). These findings suggest that the inclusion of wall-to-wall auxiliary data can reduce the costs by reducing UAV sampling intensity, while maintaining the same level of precision.

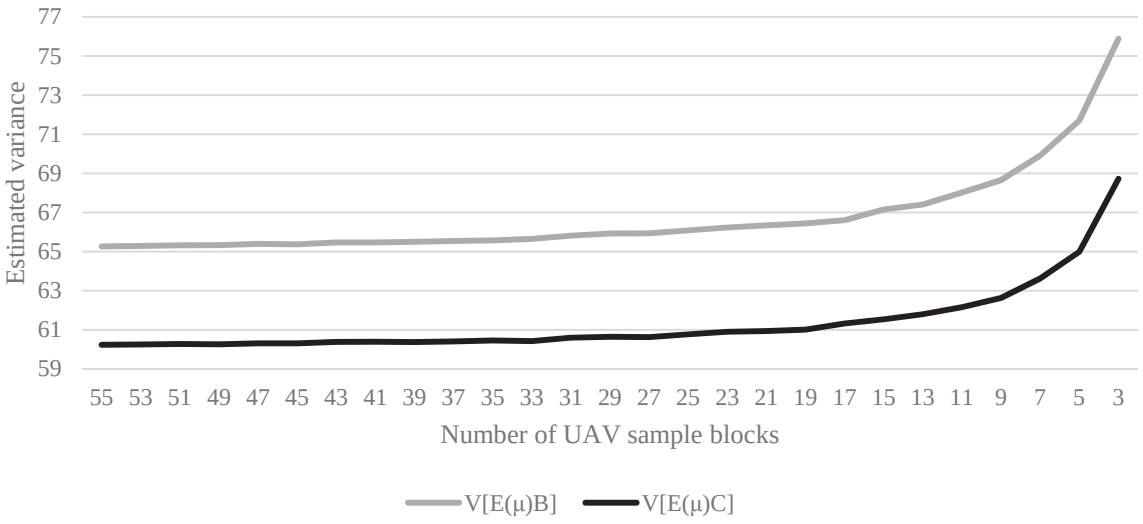

Figure 6. Averages of estimated variances for cases B ($\hat{V}\left[\widehat{E(\mu)}_B\right]$) and C ($\hat{V}\left[\widehat{E(\mu)}_C\right]$) over 6000 iterations for each UAV sample size.

The uncertainty in the model parameter estimates for the GSV~UAV model was the main source of uncertainty for case B. This was consistent in paper III (43.76 m^3 ha^{-1} or 69.7% of the estimated variance) and in paper IV (65.0 m^3 ha^{-1} or 99.6% of the estimated variance). A similar trend was observed for case C in paper IV, where the uncertainty due to the GSV~UAV model was also the main component in the estimated variance (59.9 m^3 ha^{-1} or 99.6% of the estimated variance). The contribution of this source of uncertainty was surprisingly large, however such a magnitude can possibly be explained by the fact that the sample of UAV data was rather large (i.e., approximately 20% of the entire population). Thus, it is evident that an increase in the precision of the estimation can be obtained through a reduction of the GSV~UAV model error. Some of the main factors affecting this model error relate to:

1) Small number of observations: such issue made the inference very sensitive to the choice of the second phase sample. Hence, to reduce the strong influence of few extreme observations on the uncertainty in the models' parameters larger sample sizes have to be collected. This, as suggested by Saarela et al. (2015) could ultimately result in a reduction of the GSV~UAV model error. In this regard, a major advantage in MB, HYB, and HMB comes from the possibility to include observations external to the study area. In paper III, it was demonstrated that the inclusion of field plots collected in an area contiguous to the study area can indeed lead to an increase in the precision

of the estimates. The possibility of including external observations represents an advantage in LSFS with limited budget for field data acquisition, as often is the case for UAV-based LSFS. In contrast to the RS data acquired using manned aircrafts, UAV data acquisition is more versatile for small scattered areas (i.e., field plots). Therefore, small sample sizes of field plots acquired locally can be augmented by single scattered plots acquired opportunistically or within other forest inventories (e.g., NFI).

2) RS auxiliary data used: The present thesis demonstrated that UAV photogrammetric data can be used to accurately model GSV, nevertheless smaller model errors can be expected when using laser scanning data acquired using UAVs. To date, these systems have mainly been used for research purposes as their operation costs are still high due to the hardware, software, limited flight time, and low flight altitude (i.e., small swaths at low altitudes). It is important to note that major developments in laser scanning systems are ongoing, enabled by advances made in the robotics industry. Future generations of compact laser scanning devices, or solid-state laser scanners, hold unprecedented potential for increasing the application of UAV laser scanning as a result of the limited dimensions of these sensors, the low battery consumption, and higher resolution of the data. It is possible that future applications of UAVs will be increasingly used for laser scanning data acquisition. The use of these active sensors could potentially result in a reduced GSV~UAV model error and therefore an increase in the precision of the estimation.

The cost figures for the studied cases reported in paper III were updated with figures for case C and two examples of hypothetical cases (see Table 4) were included. The first example was denoted as case C.2 and represented the previously described case C with reduced UAV sampling intensity (i.e., only five UAV blocks). The second example was denoted as case D.2 and represented case D with an increased number of field plots in order to attain the same level of precision as in case C.2. The magnitude of the factor for the increase in number of field plots was equal to the relative efficiency (RE= $\hat{V}\left[\widehat{E(\mu)}_D\right]/\hat{V}\left[\widehat{E(\mu)}_{C.2}\right]$= 4.2). Figure 7 shows the cost effectiveness of each studied case by plotting the $\widehat{SE}$ against the costs for each case. These results revealed that the lowest cost was for the acquisition of field data alone (i.e. case D). However, this came at the expense of the lowest precision of all studied cases. The cost to attain the same level of precision for case D.2 as for case C.2 was more than four times larger than for case D (i.e., 3.64 EUR ha^{-1}). As

expected, given the wall-to-wall coverage of ALS data, the largest precision was found for case A.1. The costs for this case were intermediate and it is important to mention that these costs were calculated for Norwegian conditions, where a strong market competition contributes to low prices for ALS acquisition. Larger costs can be expected for the acquisition of ALS in countries where the required technology and expertise are not readily available (i.e., developing countries). Of particular interest was the hypothetical case C.2 by which the costs could be reduced to that of case D while ensuring a precision of the estimation similar to case A.1 (i.e., wall-to-wall ALS data). Even though such a case is unrealistic in operational settings, the example showed that in case C substantial cost reductions for acquiring UAV data can possibly be achieved when including wall-to-wall Sentinel-2 data.

Table 4: Summary of estimated costs for inventory cases studied in paper III and IV.

Cost description	**Inventory costs (EUR ha^{-1})**						
	A.1	**A.2**	**B**	**C**	**C.2[a]**	**D [b]**	**D.2 [c]**
Acquisition [d]	1.48	-	3.02	1.01	0.09	0.69	2.92
Housing	-	-	0.06	0.02	0.001	0.03	0.13
Equipment [e]	-	-	0.18	0.18	0.01	0.14	0.59
Data processing [f]	-	-	0.16	0.16	0.01	-	-
Field data	0.86	0.86	0.86	0.86	0.86	-	-
Total	**2.34**	**0.86**	**4.28**	**4.28**	**0.96**	**0.86**	**3.64**

[a] case C.2 represents a hypothetical case where only 5 UAV blocks were used in a hierarchical model-based inference, i.e. the costs for acquiring UAV data were reduced by 90% compared to the full acquisition of 55 UAV blocks.
[b] Assuming that five plots (500 m^2) are measured on average each day by a team of two people.
[c] case D.2 represents a hypothetical case where only no RS data and the field plots sampling intensity was increased in order to attain the same level of precision as in case C.2.
[d] Assuming cost of labor of 61.8 EUR hour^{-1}.
[e] Transport and other running expenses.
[f] ~20 hours of work for one person.

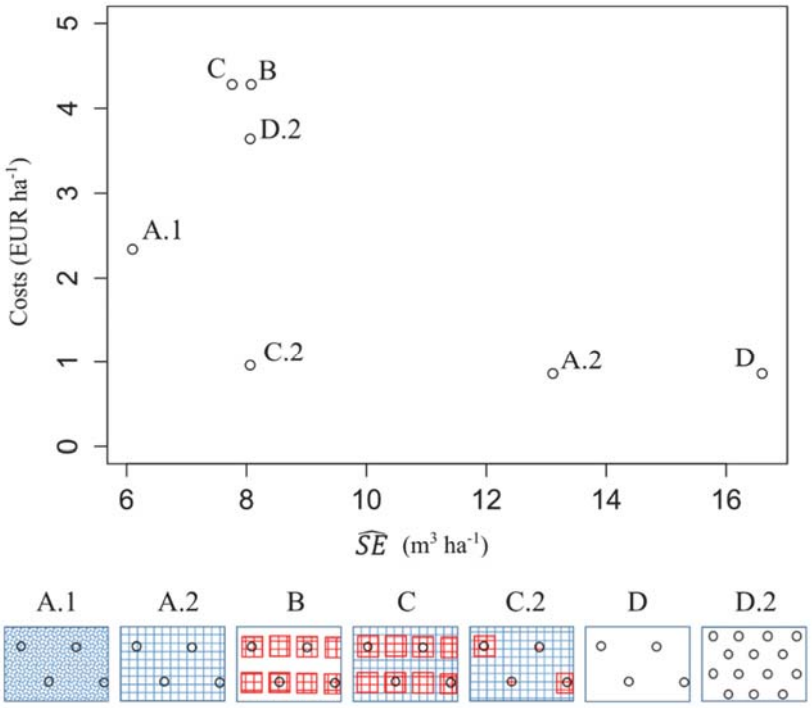

Figure 7: Scatterplot of estimated standard error ($\widehat{SE}$; m^3 ha^{-1}) against costs (EUR ha^{-1}) for each LSFS case studied. The legend shows graphically the differences between the different cases included. In addition to the cases described throughout the thesis, the following two hypothetical cases were described: case C.2 was the same of case C but the sampling intensity of UAV data was reduced to only 5 blocks, and case D.2 was the same as case D but with increased field plot sampling intensity to attain the same level of precision as for C.2.

6. Conclusion and future perspectives

6.1 Forest Management Inventories

The use of DAP in FMI is becoming an increasingly interesting application. However, it is not yet clear to what extent these data will be used operationally in future FMIs. In some countries, since ALS data is so established in operational FMI, it is likely that DAP will have more of a complementary role to ALS. On the other hand, DAP have the potential to become the main source of information for FMI in other countries because of the lower costs.

One particularly interesting application of DAP that should be addressed in the future is the use of time series of DAP canopy height models to obtain alternative sets of predictor variables to model forest biophysical properties that are otherwise difficult to model. For

instance, the use of multi-temporal CHM from DAP may provide valuable information regarding forest biophysical properties like site productivity (Véga and St-Onge 2009). This represents one of the most important variables in forest management (Eid 2000) and yet little effort has been dedicated to modelling this property. The main reason being the lack of multi-temporal CHM. Future research should therefore look into the use of CHM temporal variables from DAP for FMI, as this represents a potential operational use of DAP.

This thesis also concludes that UAV data can be used effectively in FMI in specific situations where there is a need to inventory single forest properties at specific points in time. Nevertheless, limitations to the use of UAVs for FMI were highlighted, especially in terms of the large costs for wall-to-wall acquisition. This thesis lacked an overview of the performances of UAV data across different forest development stages (i.e., only forest with mean height > 7 m were included in the studies). Nevertheless, thanks to the very high resolution of UAV data, their use may be advantageous also for regeneration forests. Therefore it would important to understand the accuracy attainable for these inventories using UAV data, as these data might outperform alternative 3D RS data sources (i.e., ALS or DAP).

6.2 Large Scale Forest Surveys

Concerning the use of UAV data for LSFS, this thesis concludes that the use of a sample of UAV data rather than wall-to-wall coverage could represent a cost-efficient application of UAVs in forest inventories. In the studied cases in this thesis (i.e., case B and C), the use of UAV data increased the precision when compared to DB estimates based on field data alone while keeping the costs of acquisition of UAV competitive to alternative RS data sources. The results of paper III and IV demonstrated that using UAVs as part of sampling strategies could be a cost-efficient solution for monitoring forest resources, especially in situations where acquisition of airborne RS data may be expensive due to the lack of technology and technical expertise (i.e., developing countries).

Paper III and IV presented case studies primarily serving illustrative purposes. Our findings should be confirmed in future studies in different forest types and adopting different sample sizes. Further research should also look into the use of case B and C to estimate a variety of forest biophysical properties using different RS auxiliary data. Particularly interesting could be to attempt to reduce the GSV~UAV model error through the use of more explanatory UAV data (e.g., laser scanning data). Furthermore, in light of the limitations

found in paper IV for moderate resolution multispectral data for GSV estimation, further studies should attempt to utilize more informative wall-to-wall auxiliary data. In this regard, space-borne canopy height models from satellite image stereo-pairs or satellite interferometric synthetic aperture radar could represent alternative sources of wall-to-wall auxiliary data.

Further research is also needed to apply methods for optimizing the sampling design both for field data and UAV data. The adoption of efficient sampling designs by spreading the samples across the auxiliary space could in fact enable a reduction in the sample sizes, hence a cost reduction. Furthermore, it is also important to mention that ongoing research is aimed at further developing the estimators. Hence, future LSFS will benefit from more advanced estimators.

6.3 Conclusion

The research done up to date clearly indicates that DAP has reached a level of maturity making it competitive with alternative 3D remote sensing data sources. The smaller cost, larger availability, and larger flexibility mean that DAP will likely play an important role in future forest inventories.

It is important to mention that the findings of this thesis assumed that an ALS DTM is available and further research should further explore the possibility to use alternative RS data sources for the generation of DTMs. One interesting approach might be to derive a DTM from the combined use of multiple sources of height information. For instance, given that photogrammetric data provides highly accurate DTMs in open areas, this information could be used to co-register coarser resolution DTMs (i.e. from satellite stereo pairs) and therefore reduce the errors that affect these types of products (Kachamba et al. 2016). Furthermore, improvements towards the generation of DTMs from photogrammetric data could be achieved from a reduction of the gaps in the data caused by shadowed areas. This could be accomplished either though flying under full cloud cover or through image processing. Further research should address the latter as the adoption of image processing algorithms prior to the photogrammetric processing (i.e., image bracketing or shadow removal algorithms) could be beneficial for the production of higher quality photogrammetric data.

The findings of this thesis were encouraging for further use of photogrammetric data both in FMI and LSFS. One important step towards the operational use of DAP in FMI is to better understand the accuracy obtainable in large area FMI and to determine the value of the

information obtained from DAP compared to ALS. Furthermore, the use of UAVs was found to be cost-effective for LSFS, nevertheless we presented some of the first results in the literature and for an operational use of the described applications, our findings should be confirmed by further studies. It is important to highlight that the LSFS applications described in this thesis are applicable to a variety of combinations of RS data sources. Hence, it is likely that future UAV assisted LSFS will benefit from future technological developments (e.g., advent of solid-state laser scanners).

References

Agisoft (2014). Agisoft Photoscan User Manual, Agisoft LLC: St. Petersburg, Russia. Available at: http://www.agisoft.com/pdf/photoscan-pro_1_1_en.pdf (29.12.2016).

Andersen, H.-E., Strunk, J., Temesgen, H., Atwood, D., & Winterberger, K. (2012). Using Multilevel Remote Sensing and Ground Data to Estimate Forest Biomass Resources in Remote Regions: A Case Study in the Boreal Forests of Interior Alaska. *Canadian Journal of Remote Sensing, 37*, 596-611.

Baltsavias, E., Gruen, A., Eisenbeiss, H., Zhang, L., & Waser, L.T. (2008). High-Quality Image Matching and Automated Generation of 3d Tree Models. *International Journal of Remote Sensing, 29*, 1243-1259.

Baltsavias, E.P. (1999). A Comparison between Photogrammetry and Laser Scanning. *ISPRS Journal of Photogrammetry and Remote Sensing, 54*, 83-94.

Bohlin, J., Wallerman, J., & Fransson, J.E. (2012). Forest Variable Estimation Using Photogrammetric Matching of Digital Aerial Images in Combination with a High-Resolution Dem. *Scandinavian Journal of Forest Research, 27*.

Boudreau, J., Nelson, R.F., Margolis, H.A., Beaudoin, A., Guindon, L., & Kimes, D.S. (2008). Regional Aboveground Forest Biomass Using Airborne and Spaceborne Lidar in Québec. *Remote Sensing of Environment, 112*, 3876-3890.

Braastad, H. (1966). Volume Tables for Birch. . *Meddr norske SkogforsVes, 21*, 23-78.

Brantseg, A. (1967). Volume Functions and Tables for Scots Pine. South Norway. *Meddr norske SkogforsVes, 22*, 689-739.

Chiao, K. (1996). Comparisons of Three Remotely Sensed Data on Forest Crown Closure and Tree Volume Estimations. *International Archives of Photogrammetry and Remote Sensing, 31*, 123-130.

Dandois, J., Olano, M., & Ellis, E. (2015). Optimal Altitude, Overlap, and Weather Conditions for Computer Vision Uav Estimates of Forest Structure. *Remote Sensing, 7*, 13895.

Dandois, J.P., & Ellis, E.C. (2010). Remote Sensing of Vegetation Structure Using Computer Vision. *Remote Sensing, 2*, 1157-1176.

Dandois, J.P., & Ellis, E.C. (2013). High Spatial Resolution Three-Dimensional Mapping of Vegetation Spectral Dynamics Using Computer Vision. *Remote Sensing of Environment, 136*, 259-276.

Eid, T. (2000). Use of Uncertain Inventory Data in Forestry Scenario Models and Consequential Incorrect Harvest Decisions. *Silva Fennica, 34*, 89-100.

Eid, T., Gobakken, T., & Næsset, E. (2004). Comparing Stand Inventories for Large Areas Based on Photo-Interpretation and Laser Scanning by Means of Cost-Plus-Loss Analyses. *Scandinavian Journal of Forest Research, 19*, 512-523.

Eid, T., & Næsset, E. (1998). Determination of Stand Volume in Practical Forest Inventories Based on Field Measurements and Photo-Interpretation: The Norwegian Experience. *Scandinavian Journal of Forest Research, 13*, 246-254.

Ene, L.T., Næsset, E., & Gobakken, T. (2016). Simulation-Based Assessment of Sampling Strategies for Large-Area Biomass Estimation Using Wall-to-Wall and Partial Coverage Airborne Laser Scanning Surveys. *Remote Sensing of Environment, 176*, 328-340.

Ene, L.T., Næsset, E., Gobakken, T., Gregoire, T.G., Ståhl, G., & Holm, S. (2013). A Simulation Approach for Accuracy Assessment of Two-Phase Post-Stratified Estimation in Large-Area Lidar Biomass Surveys. *Remote Sensing of Environment, 133*, 210-224.

Ene, L.T., Næsset, E., Gobakken, T., Gregoire, T.G., Ståhl, G., & Nelson, R. (2012). Assessing the Accuracy of Regional Lidar-Based Biomass Estimation Using a Simulation Approach. *Remote Sensing of Environment, 123*, 579-592.

Fitje, A., & Vestjordet, E. (1977). Stand Height Curves and New Tariff Tables for Norway Spruce. *Meddr norske SkogforsVes, 34*, 23-62.

Getzin, S., Nuske, R., & Wiegand, K. (2014). Using Unmanned Aerial Vehicles (Uav) to Quantify Spatial Gap Patterns in Forests. *Remote Sensing, 6*, 6988-7004.

Ginzler, C., & Hobi, M. (2015). Countrywide Stereo-Image Matching for Updating Digital Surface Models in the Framework of the Swiss National Forest Inventory. *Remote Sensing, 7*, 4343.

Gobakken, T., Bollandsås, O.M., & Næsset, E. (2014). Comparing Biophysical Forest Characteristics Estimated from Photogrammetric Matching of Aerial Images and Airborne Laser Scanning Data. *Scandinavian Journal of Forest Research*, 1-37.

Gregoire, T.G., Næsset, E., McRoberts, R.E., Ståhl, G., Andersen, H.-E., Gobakken, T., Ene, L., & Nelson, R. (2016). Statistical Rigor in Lidar-Assisted Estimation of Aboveground Forest Biomass. *Remote Sensing of Environment, 173*, 98-108.

Halbritter, K. (1996). Steps Towards a Forest Biodiversity Information System: Quantifying Forest Biodiversity by Photogrammetry and Remote Sensing Methodology. *Proceedings of International Symposium "Application of Remote Sensing in Forestry", 10*, 119-133.

Haralick, R.M., Shanmugam, K., & Dinstein, I.h. (1973). Textural Features for Image Classification. *IEEE Transactions on Systems, Man, and Cybernetics SMC-3, 6*, 610-621.

Hobi, M.L., & Ginzler, C. (2012). Accuracy Assessment of Digital Surface Models Based on Worldview-2 and Ads80 Stereo Remote Sensing Data. *Sensors, 12*, 6347.

Holmgren, J. (2004). Prediction of Tree Height, Basal Area and Stem Volume in Forest Stands Using Airborne Laser Scanning. *Scandinavian Journal of Forest Research, 19*, 543-553.

Hyyppä, J., Hyyppä, H., Inkinen, M., Engdahl, M., Linko, S., & Zhu, Y.-H. (2000). Accuracy Comparison of Various Remote Sensing Data Sources in the Retrieval of Forest Stand Attributes. *Forest Ecology and Management, 128*, 109-120.

Immitzer, M., Stepper, C., Böck, S., Straub, C., & Atzberger, C. (2016). Use of Worldview-2 Stereo Imagery and National Forest Inventory Data for Wall-to-Wall Mapping of Growing Stock. *Forest Ecology and Management, 359*, 232-246.

Järnstedt, J., Pekkarinen, A., Tuominen, S., Ginzler, C., Holopainen, M., & Viitala, R. (2012). Forest Variable Estimation Using a High-Resolution Digital Surface Model. *ISPRS Journal of Photogrammetry and Remote Sensing, 74*, 78-84.

Kachamba, D., Ørka, H., Gobakken, T., Eid, T., & Mwase, W. (2016). Biomass Estimation Using 3d Data from Unmanned Aerial Vehicle Imagery in a Tropical Woodland. *Remote Sensing, 8*, 968.

Korpela, I. (2004a). Individual Tree Measurements by Means of Digital Aerial Photogrammetry. *Sylva Fennica Monograph, 3*.

Korpela, I.A.P. (2004b). Appraisal of the Mean Height of Trees by Means of Image Matching of Digitized Aerial Photographs. *The Photogrammetric Journal of Finland, 19*.

Leberl, F.W. (1994). Practical Issues in Softcopy Photogrammetric Systems. In, *ASPRS Softcopy Photogrammetry Workshop* (pp. 223-230). Washington. Available at: http://leberl.info/sites/default/files/publications_leberl/181_-_Proctical_Issues_in_Softcopy_Photogrammetric_Systems,_ASPRS_Softcopy_Workshop,_1994.pdf.

Lisein, J., Pierrot-Deseilligny, M., Bonnet, S., & Lejeune, P. (2013). A Photogrammetric Workflow for the Creation of a Forest Canopy Height Model from Small Unmanned Aerial System Imagery. *Forests, 4*, 922-944.

Lohmann, P., Picht, G., Weidenhammer, J., Jacobsen, K., & Skog, L. (1989). The Design and Development of a Digital Photogrammetric Stereo Workstation. *ISPRS Journal of Photogrammetry and Remote Sensing, 44*, 215-224.

Lumley, T., & Miller, A. (2009). Leaps: Regression Subset Selection. Available at: http://cran.r-project.org/web/packages/leaps/leaps.pdf.

Maier, M.J. (2014). Dirichletreg : Dirichlet Regression for Compositional Data in R Dirichletreg : Dirichlet Regression for Compositional Data in R, 0.4.0; WU Vienna University of Economics and Business, Department of Statistics and Mathematics: Vienna. Available at: https://cran.r-project.org/web/packages/DirichletReg/vignettes/DirichletReg-vig.pdf.

Maltamo, M., Ørka, H.O., Bollandsås, O.M., Gobakken, T., & Næsset, E. (2014). Using Pre-Classification to Improve the Accuracy of Species-Specific Forest Attribute Estimates from Airborne Laser Scanner Data and Aerial Images. *Scandinavian Journal of Forest Research, 30*, 1-22.

Margolis, H.A., Nelson, R.F., Montesano, P.M., Beaudoin, A., Sun, G., Andersen, H.-E., & Wulder, M.A. (2015). Combining Satellite Lidar, Airborne Lidar, and Ground Plots to Estimate the Amount and Distribution of Aboveground Biomass in the Boreal Forest of North America. *Canadian Journal of Forest Research, 45*, 838-855.

McRoberts, R.E. (2006). A Model-Based Approach to Estimating Forest Area. *Remote Sensing of Environment, 103*, 56-66.

McRoberts, R.E., Andersen, H.-E., & Næsset, E. (2014a). Using Airborne Laser Scanning Data to Support Forest Sample Surveys. *Forestry Applications of Airborne Laser Scanning* (pp. 269-292): Springer.

McRoberts, R.E., Næsset, E., & Gobakken, T. (2013). Inference for Lidar-Assisted Estimation of Forest Growing Stock Volume. *Remote Sensing of Environment, 128*, 268-275.

McRoberts, R.E., Næsset, E., & Gobakken, T. (2014b). Estimation for Inaccessible and Non-Sampled Forest Areas Using Model-Based Inference and Remotely Sensed Auxiliary Information. *Remote Sensing of Environment, 154*, 226-233.

Montesano, P., Sun, G., Dubayah, R., & Ranson, K. (2014). The Uncertainty of Plot-Scale Forest Height Estimates From complementary Spaceborne Observations in the Taiga-Tundra Ecotone. *Remote Sensing, 6*, 10070-10088.

Neigh, C., Masek, J., Bourget, P., Cook, B., Huang, C., Rishmawi, K., & Zhao, F. (2014). Deciphering the Precision of Stereo Ikonos Canopy Height Models for Us Forests with G-Liht Airborne Lidar. *Remote Sensing, 6*, 1762-1782.

Neigh, C.S.R., Nelson, R.F., Ranson, K.J., Margolis, H.A., Montesano, P.M., Sun, G., Kharuk, V., Næsset, E., Wulder, M.A., & Andersen, H.-E. (2013). Taking Stock of Circumboreal Forest Carbon with Ground Measurements, Airborne and Spaceborne Lidar. *Remote Sensing of Environment, 137*, 274-287.

Nelson, R., Boudreau, J., Gregoire, T.G., Margolis, H., Næsset, E., Gobakken, T., & Ståhl, G. (2009). Estimating Quebec Provincial Forest Resources Using Icesat/Glas. *Canadian Journal of Forest Research, 39*, 862-881.

Nelson, R., Margolis, H., Montesano, P., Sun, G., Cook, B., Corp, L., Andersen, H.-E., deJong, B., Pellat, F.P., Fickel, T., Kauffman, J., & Prisley, S. (2016). Lidar-Based Estimates of Aboveground Biomass in the Continental Us and Mexico Using Ground, Airborne, and Satellite Observations. *Remote Sensing of Environment, 188*, 127-140.

Nurminen, K., Karjalainen, M., Yu, X., Hyyppä, J., & Honkavaara, E. (2013). Performance of Dense Digital Surface Models Based on Image Matching in the Estimation of Plot-Level Forest Variables. *ISPRS Journal of Photogrammetry and Remote Sensing, 83*, 104-115.

Næsset, E. (1990). Prediction of Mean Diameter, Tariff Number and Gross Value in Coniferous Stands from Aerial Photographs. In (p. 158 pp.): Norges Landbrukshøgskole (Agricultural University of). Available at: https://www.cabdirect.org/cabdirect/abstract/19940602920.

Næsset, E. (1991). Stand Volume Estimation by Means of Aerial Photographs. *Rapport fra Skogforsk (Norway)*.

Næsset, E. (2002a). Determination of Mean Tree Height of Forest Stands by Digital Photogrammetry. *Scandinavian Journal of Forest Research, 17*, 446-459.

Næsset, E. (2002b). Predicting Forest Stand Characteristics with Airborne Scanning Laser Using a Practical Two-Stage Procedure and Field Data. *Remote Sensing of Environment, 80*, 88-99.

Ota, T., Ogawa, M., Shimizu, K., Kajisa, T., Mizoue, N., Yoshida, S., Takao, G., Hirata, Y., Furuya, N., Sano, T., Sokh, H., Ma, V., Ito, E., Toriyama, J., Monda, Y., Saito, H., Kiyono, Y., Chann, S., & Ket, N. (2015). Aboveground Biomass Estimation Using Structure from Motion Approach with Aerial Photographs in a Seasonal Tropical Forest. *Forests, 6*, 3882-3898.

Packalén, P. (2009). Using Airborne Laser Scanning Data and Digital Aerial Photographs to Estimate Growing Stock by Tree Species. *Dissertationes Forestales, 77*, 41.

Packalén, P., & Maltamo, M. (2007). The K-Msn Method for the Prediction of Species-Specific Stand Attributes Using Airborne Laser Scanning and Aerial Photographs. *Remote Sensing of Environment, 109*, 328-341.

Paneque-Gálvez, J., McCall, M., Napoletano, B., Wich, S., & Koh, L. (2014). Small Drones for Community-Based Forest Monitoring: An Assessment of Their Feasibility and Potential in Tropical Areas. *Forests, 5*, 1481-1507.

Persson, H. (2016). Estimation of Boreal Forest Attributes from Very High Resolution Pléiades Data. *Remote Sensing, 8*, 736.

Persson, H., Wallerman, J., Olsson, H., & Fransson, J.E.S. (2013). Estimating Forest Biomass and Height Using Optical Stereo Satellite Data and a Dtm from Laser Scanning Data. *Canadian Journal of Remote Sensing, 39*, 251-262.

Pitt, D.G., Woods, M., & Penner, M. (2014). A Comparison of Point Clouds Derived from Stereo Imagery and Airborne Laser Scanning for the Area-Based Estimation of Forest Inventory Attributes in Boreal Ontario. *Canadian Journal of Remote Sensing, 40*, 214-232.

Puliti, S., Ene, L.T., Gobakken, T., & Næsset, E. (in submission). Use of Partial-Coverage Uav Data in Sampling for Large Scale Forest Inventories.

Puliti, S., Gobakken, T., Ørka, H.O., & Næsset, E. (2016). Assessing 3d Point Clouds from Aerial Photographs for Species-Specific Forest Inventories. *Scandinavian Journal of Forest Research, 32*, 1-40.

Puliti, S., Ørka, H.O., Gobakken, T., & Næsset, E. (2015). Inventory of Small Forest Areas Using an Unmanned Aerial System. *Remote Sensing, 7*, 9632-9654.

Rahlf, J., Breidenbach, J., Solberg, S., Næsset, E., & Astrup, R. (2014). Comparison of Four Types of 3d Data for Timber Volume Estimation. *Remote Sensing of Environment, 155*, 325–333.

Saarela, S., Holm, S., Grafström, A., Schnell, S., Næsset, E., Gregoire, T.G., Nelson, R.F., & Ståhl, G. (2016). Hierarchical Model-Based Inference for Forest Inventory Using Three Sources of Information. *Annals of Forest Science, 73*, 895-910.

Saarela, S., Schnell, S., Grafström, A., Tuominen, 821 S., Nordkvist, K., Hyyppä, J., Kangas, A., & Ståhl, G. (2015). Effects of Sample Size and Model Form on the Accuracy of Model-Based Estimators of Growing Stock Volume. *Canadian Journal of Forest Research, 45*, 1524-1534.

Seely, H.E. (1929). Computing Tree Heights from Shadows in Aerial Photography. *The Forestry Chronicle, 5*, 24-27.

senseFly (2014). Ebee Extended User Manual Available at: https://www.sensefly.com/fileadmin/user_upload/documents/manuals/Extended_User_Manual_eBee_and_eBee_Ag_v16.pdf (16.04.2016).

Sperlich, M., Kattenborn, T., & Koch, B. (2014). Potential of Unmanned Aerial Vehicle Based Photogrammetric Point Clouds for Automatic Single Tree Detection. In, *Gemeinsame Tagung 2014 der DGfK, der DGPF, der GfGI und des GiN* Available at: https://www.researchgate.net/profile/Teja_Kattenborn/publication/261643648_Potential_of_Unmanned_Aerial_Vehicle_Based_Photogrammetric_Point_Clouds_for_Automatic_Single_Tree_Detection/links/0c960534ea7ab61ef7000000.pdf.

St-Onge, B., Vega, C., Fournier, R.A., & Hu, Y. (2008). Mapping Canopy Height Using a Combination of Digital Stereo-Photogrammetry and Lidar. *International Journal of Remote Sensing, 29*, 3343-3364.

Standish, M. (1945). The Use of Aerial Photographs in Forestry. *Journal of Forestry, 43*, 252-257.

Stepper, C., Straub, C., & Pretzsch, H. (2014a). Assessing Height Changes in a Highly Structured Forest Using Regularly Acquired Aerial Image Data. *Forestry*.

Stepper, C., Straub, C., Pretzsch, H., Sensing, R., Science, Y., & Management, R. (2014b). Using Semi-Global Matching Point Clouds to Estimate Growing Stock at the Plot and Stand Levels: Application for a Broadleaf-Dominated Forest in Central Europe. *Canadian Journal of Forest Research, 45*, 111-123.

Straub, C., Stepper, C., Seitz, R., & Waser, L.T. (2013a). Potential of Ultracamx Stereo Images for Estimating Timber Volume and Basal Area at the Plot Level in Mixed European Forests. *Canadian Journal of Forest Research, 43*, 731-741.

Straub, C., Tian, J., Seitz, R., & Reinartz, P. (2013b). Assessment of Cartosat-1 and Worldview-2 Stereo Imagery in Combination with a Lidar-Dtm for Timber Volume Estimation in a Highly Structured Forest in Germany. *Forestry, 86*, 463-473.

Strunk, J.L., Temesgen, H., Andersen, H.-E., & Packalen, P. (2014). Prediction of Forest Attributes with Field Plots, Landsat, and a Sample of Lidar Strips. *Photogrammetric Engineering & Remote Sensing, 80*, 143-150.

Ståhl, G., Holm, S., Gregoire, T.G., Gobakken, T., Næsset, E., & Nelson, R. (2011). Model-Based Inference for Biomass Estimation in a Lidar Sample Survey in Hedmark County, Norway. *Canadian Journal of Forest Research, 41*, 96-107.

Taniguchi, S.-i. (1961). Forest Inventory by Aerial Photographs. *Researcg bullettins of the college experiment forest Hokkaido university, 21*, 1-80.

Tuominen, S., Balazs, A., Saari, H., Pölönen, I., Sarkeala, J., & Viitala, R. (2015). Unmanned Aerial System Imagery and Photogrammetric Canopy Height Data in Area-Based Estimation of Forest Variables. *Silva Fennica, 45*, 1348.

Vastaranta, M., Wulder, M.A., White, J.C., Pekkarinen, A., Tuominen, S., Ginzler, C., Kankare, V., Holopainen, M., Hyyppa, J., & Hyyppa, H. (2013). Airborne Laser Scanning and Digital Stereo Imagery Measures of Forest Structure : Comparative Results and Implications to Forest Mapping and Inventory Update. *Canadian Journal of Remote Sensing, 39*, 382-395.

Vauhkonen, J., Maltamo, M., McRoberts, R.E., & Næsset, E. (2014). Introduction to Forestry Applications of Airborne Laser Scanning. In M. Maltamo, E. Næsset, & J. Vauhkonen

(Eds.), *Forestry Applications of Airborne Laser Scanning* (pp. 1-16). Dordrecht, The Netherlands: Springer.

Véga, C., & St-Onge, B. (2009). Mapping Site Index and Age by Linking a Time Series of Canopy Height Models with Growth Curves. *Forest Ecology and Management, 257*, 951-959.

Vestjordet, E. (1967). Functions and Tables for Volume of Standing Trees. Norway Spruce. *Meddr norske SkogforsVes, 22*, 539-574.

Vestjordet, E. (1968). Volum Av Nyttbart Virke Hos Gran Og Furu Basert På Relativ Høyde Og Diameter I Brysthøyde Eller Ved 2,5 M Fra Stubbeavskjær [Merchantable Volume of Norway Spruce and Scots Pine Based on Relative Height and Diameter at Breast Height or 2.5 M above Stump Level]. *Meddr norske SkogforsVes, 25*, 411-459.

Wallace, L., Lucieer, A., Malenovský, Z., Turner, D., & Vopěnka, P. (2016). Assessment of Forest Structure Using Two Uav Techniques: A Comparison of Airborne Laser Scanning and Structure from Motion (Sfm) Point Clouds. *Forests, 7*, 62.

Waser, L., Fischer, C., Wang, Z., & Ginzler, C. (2015). Wall-to-Wall Forest Mapping Based on Digital Surface Models from Image-Based Point Clouds and a Nfi Forest Definition. *Forests, 6*, 4386.

Waser, L.T., Baltsavias, E., Ecker, K., Eisenbeiss, H., Feldmeyer-Christe, E., Ginzler, C., Küchler, M., & Zhang, L. (2008). Assessing Changes of Forest Area and Shrub Encroachment in a Mire Ecosystem Using Digital Surface Models and Cir Aerial Images. *Remote Sensing of Environment, 112*, 1956-1968.

White, J., Stepper, C., Tompalski, P., Coops, N., & Wulder, M. (2015). Comparing Als and Image-Based Point Cloud Metrics and Modelled Forest Inventory Attributes in a Complex Coastal Forest Environment. *Forests, 6*, 3704.

Whitehead, K., & Hugenholtz, C.H. (2014). Remote Sensing of the Environment with Small Unmanned Aircraft Systems (Uass), Part 1: A Review of Progress and Challenges. *Journal of Unmanned Vehicle Systems, 02*, 69-85.

Wulder, M. (1998). Optical Remote-Sensing Techniques for the Assessment of Forest Inventory and Biophysical Parameters. *Progress in Physical Geography, 22*, 449-476.

Yu, X., Hyyppä, J., Karjalainen, M., Nurminen, K., Karila, K., Vastaranta, M., Kankare, V., Kaartinen, H., Holopainen, M., Honkavaara, E., Kukko, A., Jaakkola, A., Liang, X., Wang, Y., Hyyppä, H., & Katoh, M. (2015). Comparison of Laser and Stereo Optical, Sar and Insar Point Clouds from Air- and Space-Borne Sources in the Retrieval of Forest Inventory Attributes. *Remote Sensing, 7*, 15809.

Zahawi, R.A., Dandois, J.P., Holl, K.D., Nadwodny, D., Reid, J.L., & Ellis, E.C. (2015). Using Lightweight Unmanned Aerial Vehicles to Monitor Tropical Forest Recovery. *Biological Conservation, 186*, 287-295.

Zhang, J., Hu, J., Lian, J., Fan, Z., Ouyang, X., & Ye, W. (2016). Seeing the Forest from Drones: Testing the Potential of Lightweight Drones as a Tool for Long-Term Forest Monitoring. *Biological Conservation, 198*, 60-69.

Ørka, H.O., Dalponte, M., Gobakken, T., Næsset, E., & Ene, L.T. (2013). Characterizing Forest Species Composition Using Multiple Remote Sensing Data Sources and Inventory Approaches. *Scandinavian Journal of Forest Research, 28*, 677-688.

Paper I Puliti, S., Gobakken, T., Ørka, H.O. & Næsset, E. 2016. Assessing 3D point clouds from aerial photographs for species-specific forest inventories. - Scandinavian Journal of Forest Research 32: 68-79. DOI: 10.1080/02827581.2016.1186727
Paper II Puliti, S., Ørka, H.O., Gobakken, T. & Næsset, E. 2016. Inventory of small forest areas using an unmanned aerial system. - Remote Sensing 7: 9632-9654. DOI: 10.3390/rs70809632
Paper III Puliti, S., Ene, L.T., Gobakken, T. & Næsset, E. Use of partial-coverage UAV data in sampling for large scale forest inventories. (Submitted)
Paper IV Puliti, S., Saarela, S., Gobakken, T., Ståhl, G. & Næsset, E. Combining UAV and Sentinel-2 auxiliary data for forest growing stock volume estimation through hierarchical model-based inference. (Manuscript)

ISBN: 978-82-575-1425-9
ISSN: 1894-6402

Norwegian University
of Life Sciences

Postboks 5003
NO-1432 Ås, Norway
+47 67 23 00 00
www.nmbu.no